Studies of oxylipin carbonyl signals under oxidative stress in triggering programmed cell death in plants

（植物での酸化ストレスによるプログラム細胞死の引き金となるオキシリピンカルボニルの研究）

Md. Sanaullah Biswas

September 2016

Studies of oxylipin carbonyl signals under oxidative stress in triggering programmed cell death in plants

（植物での酸化ストレスによるプログラム細胞死の引き金となるオキシリピンカルボニルの研究）

A thesis

Submitted to the United Graduate School of Agricultural Sciences

Tottori University

In Partial Fulfillment of the Requirements for the Degree of Doctor of Philosophy

Md. Sanaullah Biswas

September 2016

Contents

Continue

Continue

Summary

Reactive oxygen species (ROS)-triggered programmed cell death (PCD) is a typical plant response to biotic and abiotic stressors. Lipid peroxide-derived toxic carbonyl compounds (oxylipin carbonyls), products downstream of ROS, were recently revealed to mediate abiotic stress-induced damage of plants. We here investigated the biochemical mechanism by which oxylipin carbonyls triggers cell death in plant. When tobacco Bright Yellow-2 (BY-2) cells were exposed to H_2O_2, several species of short-chain oxylipin carbonyls, i.e., 4-hydroxy-(*E*)-2-nonenal and acrolein, accumulated and the cells underwent PCD as judged based on DNA fragmentation, an increase in TUNEL-positive nuclei and cytoplasm retraction. Oxylipin carbonyls caused PCD was also verified in the roots of tobacco and *Arabidopsis thaliana* after exposure with H_2O_2 and NaCl. The involvement of oxylipin carbonyls in the mediation of an oxidative signal to cause PCD, we performed pharmacological and genetic experiments. In pharmacological experiment we used carnosine and hydralazine, having distinct chemistry for scavenging carbonyls, significantly suppressed the increase in oxylipin carbonyls and blocked PCD in BY-2 cells and *A. thaliana* roots, but did not affect the levels of ROS and lipid peroxides. A transgenic tobacco line that overproduces 2-alkenal reductase, an *A. thaliana* enzyme to detoxify α,β-unsaturated carbonyls, suffered less PCD in root epidermis after H_2O_2- or NaCl treatment than did the wild type, whereas the ROS level increases due to the stress treatments were not different between the lines.

To investigate the biochemical action of oxylipin carbonyls in the cell death events we found that acrolein activated caspase-like proteases before appearing cell death morphology. We used two doses of acrolein namely lethal (0.2 mM caused PCD) and sub-lethal (0.1 mM did not cause PCD). These two doses of acrolein asserted critically different effects on the cells. Both lethal and sub-lethal doses of acrolein exhausted the cellular glutathione pool in 30 min, while lethal dose only caused a significant ascorbate decrease and ROS increase in 1-2 h.

Prior to such redox changes, we found, acrolein caused significant increases in the activities of caspase-1-like protease (C1LP) and caspase-3-like protease (C3LP), the proteases to trigger PCD. Acrolein and 4-hydroxy-(*E*)-2-nonenal, another RCS, activated both proteases in cell-free extract from untreated cells. H_2O_2 at 1 mM added to the cells increased C1LP and C3LP activities and caused PCD, and the RCS scavenger carnosine suppressed their activation and PCD. However, H_2O_2 did not activate the proteases in cell-free extract. We also found that acrolein after 30 min exposure slightly but insignificantly up-regulated *VPE1a, VPE1b* genes, attribute to C1LP, although the up-regulation was significant after 1 h. Therefore, the activation of caspase-like proteases by RCS was the most critical and initial biochemical event in oxidative signal-simulated PCD in plants.

From these results we conclude that oxylipin carbonyls, downstream product of ROS, are involved in the PCD process in oxidatively stressed cells. We estimated the relative strengths of distinct carbonyl species and found that acrolein and 4-hydroxy-(*E*)-2-nonenal are the most potent carbonyls. Acrolein activated caspase-like proteases before changes the redox state of the cells. These results reveal the biochemical mechanisms of the oxylipin carbonyls-mediated initiation of PCD in plants. Our findings demonstrate a critical role of the lipid metabolites oxylipin carbonyls in ROS signaling.

Chapter 1

General Introduction

1.1 Programmed cell death in plants

Cell death is an essential fate of all living organism during normal growth and development. The term programmed cell death (PCD) was introduced to indicate an active cell suicide displaying different feature from necrosis. PCD is a controlled and organized destruction of cells, while necrosis is a chaotic and uncontrolled mode of death. A single or series of biochemical and molecular changes become visible in cells during PCD program but necrosis results from severe and persistent trauma that is considered not to be genetically orchestrated (Gadjev *et al.,* 2008). In the animal research field, three different types of PCD have been recognized: apoptosis, autophagy and less characterized necrosis-like. Apoptosis was the first form of PCD reported in animal process thus plant PCD has often been investigated in comparison to the apoptosis. Although plant cell death shares some similarities with animal cell death, during PCD process both kingdoms show some obvious differences. This distinctive feature is probably due to the presence of the cell wall and the absence of phagocytosis in plants. For instance, in plant PCD, cell condensation is evident as a cytoplasmic shrinkage in which the plasma membrane separates from the cell wall (Reape and McCabe, 2013), but it is not accompanied by cell fragmentation and formation of the so-called cellular apoptotic bodies, which is characterize apoptosis in animals (van Doorn *et al.,* 2011). Nuclear and chromatin condensation, as well as DNA laddering, are apoptosis hallmarks also found in several forms of plant PCD (Vacca *et al.* 2004; Locato *et al.* 2006). Therefore, it has been concluded that in plants, as in animals, a variety of biochemical and genetic pathways are involved in different forms of PCD often overlaps.

1.1.1 Cell death in stress responses

PCD can be manifested in higher plants as their adaptation strategies under different

stressful conditions. For example, salt stress disturb water as well as nutrient uptake of the terrestrial or aquatic plants leading to plant growth inhibition and even death (Tuteja 2007). High temperature hamper homeostatic limits and also results in cell death (Zhang *et al.* 2011). Terrestrial plant tolerates low-oxygen environments by the degradation of certain parenchymatic cells of root apex for the formation of aerenchyma also triggered by PCD. Plant pathogen attack can also induce PCD at the infection sites through a mechanism known as hypersensitive response (HR) (de Pinto *et al.* 2012). In this HR mechanism plants limit pathogen spreading and avoid greater damage and even prevent the death of the entire plant.

1.1.2 Cell death in plant growth and development

During growth and development process plants remove the cells that are ultimately unnecessary or damaged beyond repair by the PCD process (Williams and Dickman, 2008, Reape & McCabe, 2008). It is essential to maintain their growth and developments such as development of endosperm and aleurone cells in cereals and storage tissues (Lombardi et al. 2010), differentiation of tracheary elements (Cho & Park, 2010), female gametophyte differentiation (Wu & Cheung, 2000), leaf and flower abscission (Bar-Dror et al., 2011) and whole plant senescence (Lee et al., 2011). Thus PCD process is indispensible for successful vegetative and reproductive development of plants.

1.2 Production of reactive oxygen species (ROS) and antioxidants defense

ROS are constitutively produced in cell of normal metabolism in aerobic organisms. Being plant is an aerobic organisms and therefore utilizes molecular oxygen (O_2) as a terminal electron acceptor. After incomplete reduction of O_2 reactive oxygen species (ROS) are generated as a bi-product. In chloroplast and mitochondria, the major parts of the production of ROS are associated with their electron transport chains residing in the thylakoid membrane and the inner membrane, respectively (Mano, 2012). ROS levels are maintained at constant basal levels in healthy cells, but their levels transiently or persistently increase under different

stress conditions or in response to developmental signals (Gechev et al. 2006). As plant face burden of excess ROS, they are equipped with abundant antioxidant molecules such as α-tocopherol, β-carotene and ascorbic acid and an array of ROS-scavenging enzymes such as superoxide dismutase and ascorbate peroxidase, to maintain low intracellular ROS levels. In severe or prolonged exposure of plants to environmental stress, the balance between the production and scavenging of ROS is disrupted, and the cellular metabolism reaches a new state of higher ROS production and lower antioxidant capacity, leading to cell death (Mano 2002). In response to attack by pathogens including bacteria, fungi and viruses, the infected cells produce transiently as 'oxidative burst' via the activation of the respiratory burst oxidase homologs (Levine et al. 1994, Torres and Dangl 2005). This type of ROS formation leads to death of the original and neighboring cells and induces defense responses in the surrounding uninfected cells (Torres et al. 2005). These various effects of ROS are collectively designated as oxidative signaling (Mittler et al. 2011).

1.3 Involvement of ROS in cell death

PCD is one of the typical consequences of oxidative signaling (Van Breusegem and Dat 2006, Petrov et al. 2015). For example, in tobacco (*Nicotiana tabacum*) Bright Yellow-2 (BY-2) cells, an increase in the O_2^- level is necessary for execution of PCD on salt and sorbitol stress (Monetti et al. 2014). Short-term drought on developing anthers in rice (*Oriza sativa*) increases the level of H_2O_2 and decreases the level of transcripts of antioxidant enzymes, and thereby leads to PCD (Nguyen et al. 2009). High temperature treatment of tobacco cells increases the H_2O_2 level before PCD occurs (Locato et al. 2008). NaCl treatment activates the plasma membrane NADPH oxidases to facilitate superoxide production, from which H_2O_2 is formed via catalysis with superoxide dismutase. NaCl treatment also activates polyamine oxidase, which catalyzes the production of H_2O_2 in the oxidation of spermine and spermidine. Thus NaCl treatment also imposes H_2O_2 stress on plant cells (Petrov et al., 2015). Hypersensitive response (HR)-like cell death, a typical PCD in tobacco leaves, is also caused

by H_2O_2 (Yoda et al. 2003).

1.4 Proteases regulate cell death in plant

PCD is a central component of the plant immune response and its importance for plant life is uncontested. However, in comparison to the state-of-the-art study of animal PCD, most prominently apoptosis, plant PCD research is emerging recently. In animals, the activation of caspase proteases, a group of ubiquitously expressed cysteine proteases, is the regulator of PCD. In the caspase activation process, a proteolytic cascade function is started by initiator caspases and activated by executor caspases. Resulting active caspases degrade a variety of target proteins and trigger cell death program (Shi 2004, Hengartner 2000). In plants proteases also play a key role in PCD, as in animals. However, plant genomes do not encode caspases, but a variety of caspase-like activities have been typically associated in plant cell death process. Various proteases in plant show caspase-like activities such as metacaspase, phytaspase, saspases, vacuolar processing enzymes (VPE; also known as legumain) and the proteasomes. Among these proteases VPEs and the subunit PBA1 of the proteasome have been largely characterized during stress-stimuli, and developmental process featuring cell death. VPEs and the subunit PBA1 of the proteasome were active against caspase-1 substrate and caspaspe-3 substrate and were blocked by their inhibitors, similar to their mammalian counterparts. The contribution of caspase-1-like protease (C1LP) to plant PCD compares with the animal caspase-1 as a cell death executor (Hatsugai et al. 2015). Caspase-3-like protease (C3LP) activity is involved in HR-induced or abiotic stress-regulated PCD (Fernández et al. 2012, Ye et al. 2013) and can be attributed to the 20S proteasome subunit PBA1 (Han et al. 2012, Hatsugai et al. 2009).

1.5 Biochemical mechanisms of ROS action to the cell death induction

The above mentioned ROS-induced cell death are the results of oxidative signals (Gechev *et al.,* 2006; Van Breusegem and Dat, 2006). Since H_2O_2 can be involved in different

environmental and developmental responses, as well as in PCD, an interesting question is how this small molecule controls so many different processes. The identification of genes responding to elevated H_2O_2 levels and mutants deficient for H_2O_2 signaling pathway has led to a better understanding of how the ROS-signaling network functions. A vast network of mitogen-activated protein kinases (MAPK) is also involved during PCD that is triggered by chloroplast-derived H_2O_2 in plants (Liu *et al.,* 2007). Nucleotide diphosphate kinases and protein phosphatases are other components of the H_2O_2 signaling network (Schweighofer *et al.,* 2004). Finally, the H_2O_2 signaling network transmits the signal to ROS-specific transcription factors that then regulate gene expression and lead to activation of the H_2O_2-dependent cell death (Gadjev et al., 2006). However, interaction of ROS with other signaling molecules such as lipids and hormones to start signaling events is largely unknown in plants.

1.6 Involvement of oxylipin carbonyls in oxidative signaling

1.6.1 Production of RCS from lipids

Photosynthetic electron transport chains residing on the thylakoid membrane and the inner membrane of plant cells are major source of ROS. On the other hand, membrane lipids are the most abundant molecules in the membranes and hence the most probable targets of ROS. Oxidation of lipids occurs at their fatty acids, especially polyunsaturated fatty acids (PUFA) such as linoleic acid and linolenic acid. Singlet oxygen ($^1O_2$) attacks double bond of PUFA to form an endoperoxide, and then converts to a hydroperoxide. Under light stress condition, plant leaf cells produce LOOH in this mechanism. Alternatively, hydroxyl radical ($HO^{\bullet}$) and superoxide radical (protonated form; $HO^{\bullet}_2$) abstract a hydrogen atom from a double bond on a PUFA. The resulting radical of PUFA is stabilized at the central carbon of the pentadienyl structure, to which O_2 is attached to form a peroxyl radical. This is the initiation reaction of the chain reaction to form LOOH (Mano 2012). Then carbonyl compounds are produced from lipid peroxides by the catalysis with radical species or redox catalysts. In the presence of

transition metal ions and reductants, LOOH is converted via the Fenton mechanism to a highly reactive alkoxyl radical, which readily oxidize neighbouring lipids to form lipid radicals and lipid peroxyl radicals. Carbonyl species are produced from these alkoxyl and peroxyl radicals via their spontaneous decomposition. Among the many different carbonyls, which those contain the α,β-unsaturated bond have high reactivity and hence termed as reactive carbonyl species (RCS).

1.6.2 Occurrence of oxylipin carbonyls in plants

The presence of RCS in plant cells is getting emphasis in the recent days considering its reactivity with various cellular components. Aldehyde analysis of unstressed plant tissues revealed the occurrence of RCS such as acrolein and 4-hydroxy-(*E*)-2-hexenal (HHE) and their levels increase in stressed plants (Mano *et al.,* 2010). For instance, $AlCl_3$ treatment markedly increased the contents of highly reactive acrolein, 4-hydroxy-(*E*)-2-nonenal (HNE), HHE and other aldehydes in the wild type tobacco roots (Yin *et al.* 2010). The formation of HNE was also observed in association with Al treatment in barley (*Hordeum vulgare*) roots (Sakihama and Yamasaki, 2002). The occurrence of HNE in Arabidopsis cultured cells under oxidative stress has been also deduced by detection of modified proteins in the mitochondria (Winger *et al.,* 2007). Thus, endogenous occurrence of various RCS in plant cells is a common event in oxidative-stressed plant cells.

1.6.3 Action of oxylipin carbonyls on cellular functions and components

It is now recognized in animal cells that the toxicity of LOOH is largely ascribable to LOOH-derived aldehydes. In particular, RCS, such as acrolein and HNE are strong electrophiles and readily modify proteins and nucleic acids (Esterbauer *et al.,* 1991; Taylor *et al.,* 2002; O'Brien *et al.,* 2005; Møller *et al.,* 2007). RCS form Michael adducts with nucleophiles such as cysteine, lysine and histidine residues on proteins and nucleic acid base such as guanine and also form a Schiff-base with the amino group. HNE rapidly inhibited

respiration in isolated potato mitochondria by inactivating pyruvate dehydrogenase, 2-oxoglutarate dehydrogenase, NAD-malic enzyme (Millar and Leaver, 2000), and alternative oxidase (Winger et al., 2005). HNE and other RCS also inactivated photosynthesis in isolated chloroplasts (Mano *et al.,* 2009). HNE also reacted with specific sites in mitochondrial proteins, leading to diverse changes in protein function and/or stability (Winger *et al.,* 2007). OEC33 protein in photosystem II and light-harvesting chlorophyll-binding proteins were preferentially modified by RCS of in heat-stressed leaves (Yamauchi *et al.,* 2008). Thus, the above mentioned literature indicates that the reactions of RCS with various cellular components are inevitable in plants.

1.6.4 Evidence that RCs are involved in the environmental stress-induced damages in plants

The involvement of RCS in cellular damage has been demonstrated by the protective effects of the aldehyde scavenging enzymes aldehyde dehydrogenase (ALDH) (Sunkar *et al.,* 2003; Kotchoni *et al.,* 2006) and aldehyde reductase (Oberschall *et al.,* 2000; Hideg *et al.,* 2003; Hegedüs *et al.,* 2004); 2-alkenal reductase (AER) (Mano et al., 2002) to confer tolerance against various environmental stresses when they were overexpressed in plants. For example, AER-overproducing tobacco showed tolerance to strong light and to methyl viologen (Mano *et al.,* 2005), and to aluminum (Yin *et al.,* 2010) and Arabidopsis showed tolerance to NaCl (Papdi *et al.,* 2008). Transgenic *A. thaliana* also show stress tolerance to NaCl and heavy metals when overexpressed ALDH (Sunker et al. 2003). Therefore, underlying the above facts, it is obvious that RCS are involved in stress-induced damages in plants.

1.7 Purpose of this study

Under stressful condition, plant generate excess ROS which leads to oxidative stress that restrict plant growth and development or even death. In response to oxidative stress, plants employ PCD as of their defense strategy. The enhance levels of ROS in oxidative stress trigger PCD. However, the biochemical processes between the generation of ROS and cell death are poorly understood. Therefore, the purpose of this study were (1) to verify the hypothesis whether LOOH-derived oxylipin carbonyls, downstream products of ROS, are involved in cell death in plants; and (2) to investigate the mechanism by which oxylipin carbonyls initiate PCD. Our findings suggest that oxylipin carbonyls are involved in the PCD process, and oxylipin carbonyls induced activation of caspase-like protease is an initial biochemical event in oxidatively stressed PCD in plants.

Chapter 2

Lipid peroxide-derived short-chain carbonyls mediate H_2O_2-induced and NaCl-induced programmed cell death in plants

2.1 Abstract

Lipid peroxide-derived toxic carbonyl compounds (oxylipin carbonyls), produced downstream of reactive oxygen species (ROS), were recently revealed to mediate abiotic stress-induced damage of plants. We here investigated how oxylipin carbonyls cause cell death. When tobacco Bright Yellow-2 (BY-2) cells were exposed to H_2O_2, several species of short-chain oxylipin carbonyls, i.e., 4-hydroxy-(*E*)-2-nonenal and acrolein, accumulated and the cells underwent programmed cell death (PCD) as judged based on DNA fragmentation, an increase in TUNEL-positive nuclei and cytoplasm retraction. These oxylipin carbonyls caused PCD in BY-2 cells and roots of tobacco and *Arabidopsis thaliana*. To test the possibility that oxylipin carbonyls mediate an oxidative signal to cause PCD, we performed pharmacological and genetic experiments. Carnosine and hydralazine, having distinct chemistry for scavenging carbonyls, significantly suppressed the increase in oxylipin carbonyls and blocked PCD in BY-2 cells and *A. thaliana* roots, but did not affect the levels of ROS and lipid peroxides. A transgenic tobacco line that overproduces 2-alkenal reductase, an *A. thaliana* enzyme to detoxify α,β-unsaturated carbonyls, suffered less PCD in root epidermis after H_2O_2- or NaCl treatment than did the wild type, whereas the ROS level increases due to the stress treatments were not different between the lines. From these results we conclude that oxylipin carbonyls are involved in the PCD process in oxidatively stressed cells. Our comparison of distinct carbonyls' ability to induce PCD in BY-2 cells revealed that acrolein and 4-hydroxy-(*E*)-2-nonenal are the most potent carbonyls. The physiological relevance and possible mechanisms of the carbonyl-induced PCD are discussed.

2.2 Introduction

In plants, environmental stressors such as extreme temperatures, drought, intense UV-B radiation, and soil salinity can cause tissue damage, growth inhibition and even death. These detrimental effects are often ascribed to the action of reactive oxygen species (ROS) produced in the stressed plants, for the following reasons: (i) Various environmental stressors commonly cause the oxidation of biomolecules in plants, and (ii) transgenic plants with enhanced antioxidant capacities show improved tolerance to environmental stressors (Suzuki et al., 2014). Production of ROS such as superoxide anion radical and hydrogen peroxide (H_2O_2) is intrinsically associated with photosynthesis and respiration (Foyer and Noctor, 2003; Asada, 2006).

Plant cells are equipped with abundant antioxidant molecules such as α-tocopherol, β-carotene and ascorbic acid and an array of ROS-scavenging enzymes such as superoxide dismutase and ascorbate peroxidase, to maintain low intracellular ROS levels. When plants are exposed to severe and prolonged environmental stress, the balance between the production and scavenging of ROS is disrupted, and the cellular metabolism reaches a new state of higher ROS production and lower antioxidant capacity. Then oxidation of vital biomolecules such as proteins and DNA proceeds, and as a consequence, cells undergo oxidative injury (Mano, 2002). The cause-effect relationship between ROS and tissue injury in plants is thus widely accepted, but the biochemical processes between the generation of ROS and cell death are poorly understood.

Increasing evidence shows that oxylipin carbonyls mediate the oxidative injury of plants (Yamauchi et al., 2012; reviewed by Mano, 2012 and Farmer and Mueller, 2013). Oxylipin carbonyls are a group of carbonyl compounds derived from oxygenated lipids and fatty acids. The production of oxylipin carbonyls in living cells is explained as follows. Lipids in the membranes are constitutively oxidized by ROS to form lipid peroxides (LOOH)

(Mène-Saffrané et al., 2007) because they are the most immediate and abundant targets near the ROS production sites. There are two types of LOOH formation reaction from ROS (Halliwell and Gutteridge, 2007). One is the radical-dependent reaction. Highly oxidizing radicals, i.e., hydroxyl radical (standard reduction potential of the $HO^{\bullet}/H_2O$ pair, +2.31 V) and the protonated form of superoxide radical (HO_2/H_2O_2, +1.06 V) can abstract a hydrogen atom from a lipid molecule, especially at the central carbon of pentadiene structure in a polyunsaturated fatty acid, to form a radical. This organic radical rapidly reacts with molecular oxygen, forming a lipid hydroperoxyl radical, which then abstracts a hydrogen atom from a neighboring molecule and becomes a LOOH. The other reaction is the addition of singlet oxygen to a double bond of an unsaturated fatty acid to form an endo-peroxide, or a hydroperoxide (both are LOOH). A variety of LOOH species are formed, depending on the source fatty acid and also by the oxygenation mechanism (Montillet et al., 2004). LOOH molecules are unstable, and in the presence of redox catalysts such as transition metal ions or free radicals, they decompose to form various aldehydes and ketones, i.e., oxylipin carbonyls (Farmer and Mueller, 2013). The chemical species of oxylipin carbonyl formed in the cells differ according to the fatty acids and the type of ROS involved (Grosch, 1987; Mano et al., 2014a).

More than a dozen species of oxylipin carbonyls are formed in plants (reviewed by Mano et al., 2009). Oxylipin carbonyls are constitutively formed in plants under normal physiological conditions, and the levels of certain types of oxylipin carbonyls rise by several-fold under stress conditions, detected as increases in the free carbonyl content (Mano et al., 2010; Yin et al., 2010; Kai et al., 2012) and by the extent of the carbonyl-modification of target proteins (Winger et al., 2007; Mano et al., 2014b). Among the oxylipin carbonyls, the α,β-unsaturated carbonyls such as acrolein and 4-hydroxy-(*E*)-2-nonenal (HNE) have high reactivity and cytotoxicity (Esterbauer et al., 1991; Alméras et al., 2003). They strongly inactivate lipoate enzymes in mitochondria (Taylor et al., 2002) and thiol-regulated enzymes

in chloroplasts (Mano et al., 2009) *in vitro* and cause tissue injury in leaves when they are fumigated (Matsui et al., 2012).

The physiological relevance of oxylipin carbonyls has been shown by the observation that the overexpression of different carbonyl-scavenging enzymes commonly confers stress tolerance to transgenic plants (reviewed by Mano 2012). For example, 2-alkenal reductase (AER)-overproducing tobacco showed tolerance to aluminum (Yin et al., 2010); aldehyde dehydrogenase-overproducing *Arabidopsis thaliana* showed tolerance to osmotic stress and to oxidative stress (Sunker et al., 2003), and aldehyde reductase-overproducing tobacco showed tolerance to chemical and drought stress (Oberschall et al., 2000). In addition, the genetic suppression of a carbonyl-scavenging enzyme made plants susceptible to stresses (Kotchoni et al., 2006; Shin et al., 2009; Yamauchi et al., 2012; Tang et al., 2014). Under stress conditions, there are positive correlations between the level of certain carbonyls and the extent of tissue injury (Mano et al., 2010; Yin et al., 2010; Yamauchi et al., 2012). Thus it is evident that oxylipin carbonyls, downstream products of ROS, are causes of oxidative damage of plant cells.

To investigate how oxylipin carbonyls damage cells in oxidative-stressed plants, we here examined the mode of cell death that is induced by oxylipin carbonyls, and we identified the carbonyl species responsible for the cell death. We observed that oxylipin carbonyls cause programmed cell death (PCD), and our results demonstrated that the oxylipin carbonyls mediate the oxidative stress-induced PCD in tobacco Bright Yellow-2 (BY-2) cultured cells, and in roots of tobacco and *A. thaliana* plants. We then estimated the relative strengths of distinct carbonyl species to initiate the PCD program. Our findings demonstrate a critical role of the lipid metabolites in ROS signaling.

2.3 Results

2.3.1 Oxylipin carbonyls formed in H_2O_2-stressed cells can cause PCD

To investigate the process of oxidative injury in plant cells, we first used tobacco BY-2 cells and gave them an oxidative stimulus with H_2O_2. Cells that underwent a 4-d culture (0.7 g fresh weight per flask) propagated to double weight in approx. 20 h under the normal culture conditions (Fig. 1A, untreated). When H_2O_2 was added to 1 mM, the cells stopped propagation and their fresh weight started to decrease. At 20 h, the fresh weight was reduced to 0.4 g (Fig. 1A) and the cells were apparently dead, as detected by trypan-blue staining (Fig. 1B,C).

H_2O_2 induces PCD in BY-2 cells, appearing as morphological changes and nuclear DNA fragmentation (Houot et al., 2001). We also detected PCD-associated events in the BY-2 cells in the 20-h H_2O_2-treatment group, as follows: (1) The fragmentation of genomic DNA into 0.18 kb and its multiples was detected as DNA laddering (Fig. 2A). (2) More than 80% of the cells had positive nuclei in the terminal deoxynucleotidyl transferase dUTP nick end labeling (TUNEL) assay, which represents the fragmentation of DNA, whereas <2% of the untreated control cells were positive (Fig. 2B). (3) Retraction of cytosol from the cell wall (Reape and McCabe, 2008) was observed (Fig. 2D). Thus under our experimental conditions, too, H_2O_2 induced PCD in BY-2 cells.

According to our previous observations of tobacco leaves and roots (Mano et al., 2010; Yin et al., 2010), oxidative stress treatment will increase the levels of oxylipin carbonyls before apparent cell death is observed. At 2 h after treatment, when the H_2O_2-treated cells had just stopped growth (Fig. 1A), we extracted carbonyls from the cells, derivatized them with 2,4-dinitrophenylhydrazine and analyzed them by HPLC. Eight species of carbonyls of C1-C9 were detected in the untreated cells (Fig. 3A). In the H_2O_2-treated cells, the levels of HNE, *n*-hexanal, *n*-heptanal, malondialdehyde, acetaldehyde and propionaldehyde were

significantly higher (Fig. 3B). Acrolein and HHE also tended to be higher in the H_2O_2-treated cells, although the difference was not significant.

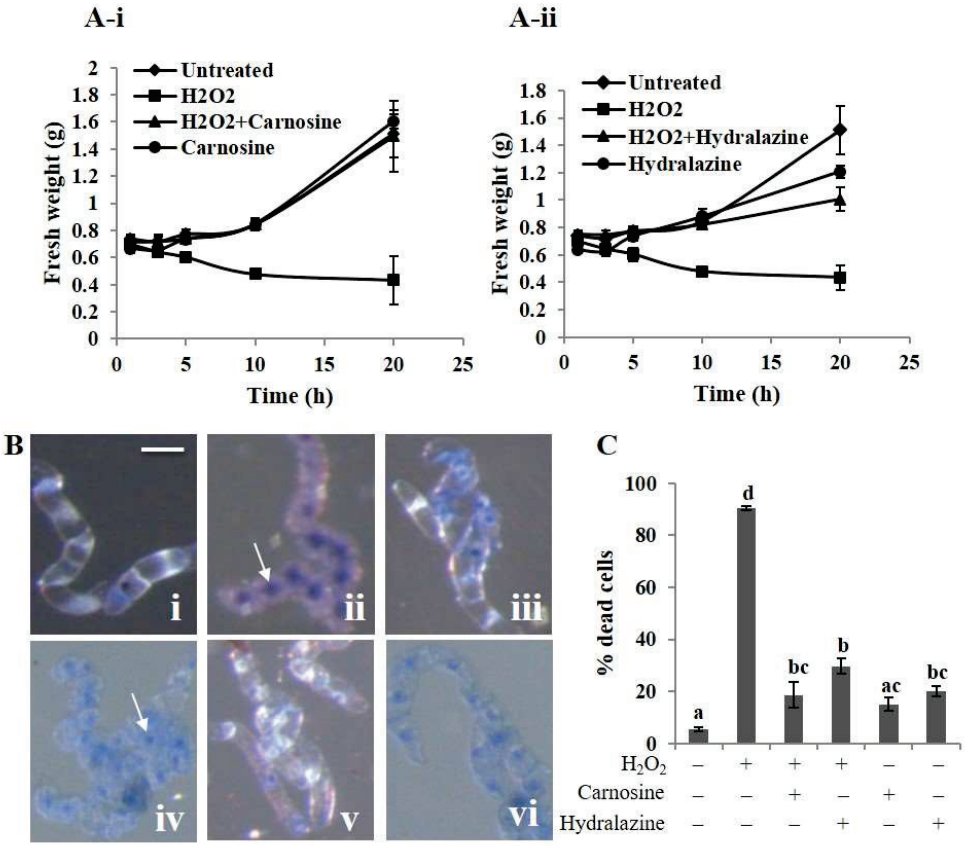

Fig. 1. Carnosine and hydralazine suppressed the H_2O_2-induced growth inhibition and cell death of tobacco Bright Yellow-2 (BY-2) cells. Fifty milligrams of cells from 7-d culture were subcultured in 50 mL fresh culture media, and after 4 d the culture medium was supplemented with either 1 mM H_2O_2 or a carbonyl scavenger (1 mM carnosine or 0.2 mM hydralazine) or both. (A) Changes in the fresh weight (per flask) of cells. Cells were collected at the indicated time points and weighed immediately. Carnosine (panel A-i) and hydralazine (A-ii) were included as indicated. Mean ± SEM of three independent experiments. (B) Detection of cell death with trypan-blue staining. BY-2 cells treated as in (A) were collected at 20 h and stained as described in Materials and Methods. Cells forming a single layer under microscopy were chosen for the evaluation. Typical images of the trypan-blue staining are shown: (i) untreated cells as blank control, (ii) 1 mM H_2O_2, (iii) 1 mM H_2O_2 + 1 mM carnosine, (iv) 1 mM H_2O_2 + 0.2 mM hydralazine, (v) 1 mM carnosine and (vi) 0.2 mM hydralazine. White arrows indicate dead cells. Bar, 50 μm. (C) The fraction of dead cells (trypan blue-stained cells) at 20-h incubation. A total of 200 cells were counted in each treatment. Mean ± SEM of three independent experiments. Differences among treatments were analyzed by Tukey test. $P<0.05$.

We also determined carbonyls at 5 h (Supplemental Fig. S1), when the H_2O_2-treated cells showed a notable loss of fresh weight. Highly electrophilic and reactive carbonyls such as HNE and HHE were significantly increased and other less reactive saturated carbonyls such as *n*-hexanal and *n*-heptanal were increased by at least 10-fold compared to the 2 h-treated cells (Suppl. Fig. S2). It should be noted that the *α,β*-unsaturated carbonyls HNE and acrolein were increased by the H_2O_2 treatment at an early stage and continued to increase afterward. These compounds can induce cell death in animals (Kruman et al., 1997; Liu-Snyder et al., 2006) and cause tissue injury in plants (Alméras et al., 2003, Mano et al., 2005; Yin et al., 2010; Kai et al., 2012).

We tested the ability of acrolein, HNE, *n*-hexanal, *n*-heptanal, (*Z*)-3-hexenal and propionaldehyde to cause PCD in BY-2 cells. The addition of acrolein (Fig. 4) and HNE (Suppl. Fig. S3) at 0.2 mM and *n*-hexanal (Suppl. Fig. S4) at 3 mM to the cells resulted in DNA laddering, an increase in the percentage of TUNEL-positive nuclei, and cytoplasm retraction. DNA laddering was also found with 3 mM *n*-heptanal, 3 mM (*Z*)-3-hexenal and 50 mM propionaldehyde (Suppl. Fig. S10). These carbonyl concentrations required for inducing PCD were clearly higher than their endogenous levels. This is probably because exogenously added carbonyls were first scavenged by the cell with glutathione and specific enzymes, and the residual unscavenged carbonyls exerted cytotoxicity or signaling actions.

2.3.2 Carbonyl scavengers suppressed the intracellular carbonyls and the H_2O_2-induced PCD

We hypothesized that if oxylipin carbonyls formed after H_2O_2 treatment are responsible for the PCD, the scavenging of them would stop the cell death. To test this hypothesis, we used two carbonyl-scavenging agents—carnosine and hydralazine—and examined their effects on the death of the H_2O_2-treated cells. Carnosine is a dipeptide (*β*-alanyl-L-histidine) found in skeletal muscles and brain in vertebrates at millimolar levels. It can covalently trap

carbonyls at the amino end of its β-alanyl moiety (Aldini et al., 2002; Burcham et al., 2002). Hydralazine (1-hydrazinylphthalazine) can trap carbonyls at its hydrazine moiety (Burcham et al., 2002).

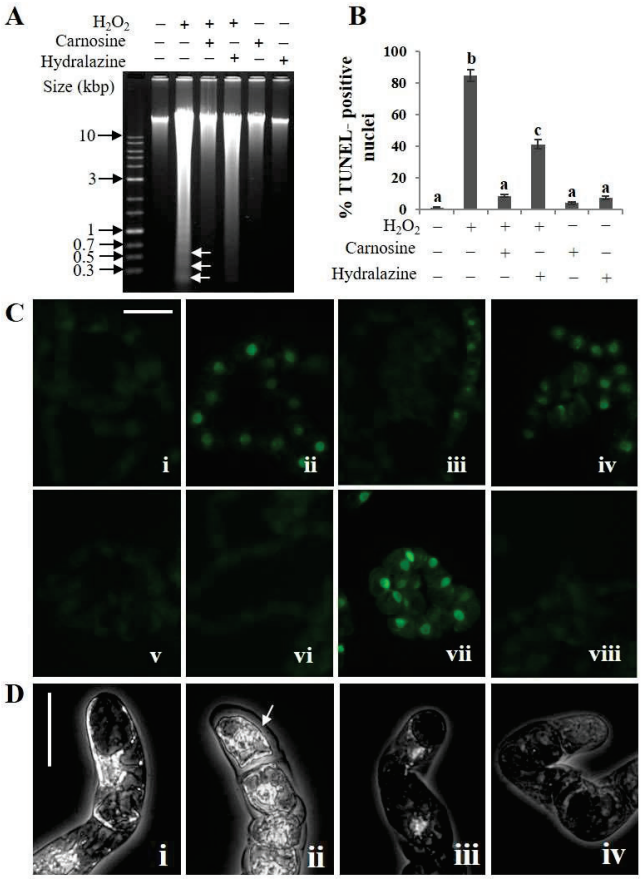

Fig. 2. PCD-associated events in BY-2 cells induced by H_2O_2 were suppressed by RCS scavengers. Four-d-cultured cells were treated with 1 mM H_2O_2 with or without a carbonyl scavenger (1 mM carnosine or 0.2 mM hydralazine). After a 20-h incubation, the cells were used for genomic DNA extraction, a TUNEL assay and cytoplasm retraction observation as described in Materials and Methods. (A) Agarose gel electrophoresis of genomic DNA. Cells were treated as indicated at the top of each lane. The leftmost lane is for molecular weight markers. White arrows indicate the DNA fragments of 0.18, 0.36 and 0.54 kbp. (B) Fraction of the cells with TUNEL-positive nuclei. Cells forming a single layer under microscopy were chosen for the evaluation. The total cell number was counted under phase contrast observation, and the TUNEL-positive cells were counted under fluorescence observation. All values are mean ± SEM, and the data represent three independent experiments. Differences among treatments were analyzed by Tukey test. $P<0.05$. (C) Typical fluorescence microscopy images of the TUNEL assay results: (i) untreated cells as blank control, (ii) 1 mM H_2O_2, (iii) 1 mM H_2O_2 + 1 mM carnosine, (iv) 1 mM H_2O_2 + 0.2 mM hydralazine, (v) 1 mM carnosine, (vi) 0.2 mM hydralazine, (vii) positive control and (viii) negative control. Bar, 50 µm. (D) Typical phase-contrast microscopy images of cell morphology for cytoplasm retraction: (i) untreated control cells, (ii) 1 mM H_2O_2, (iii) 1 mM H_2O_2 + 1 mM carnosine, and (iv) 1 mM H_2O_2 + 0.2 mM hydralazine. Bar, 50 µm.

Our findings confirmed that carnosine and hydralazine suppressed the carbonyl-induced PCD. When carnosine (1-5 mM) or hydralazine (0.2 mM) was added with acrolein, HNE, *n*-hexanal, *n*-heptanal, (*Z*)-3-hexenal or propionaldehyde in the culture medium, all of the PCD-associated events caused by these aldehydes were suppressed; i.e., the DNA laddering (Fig. 4A; Suppl. Figs. S3A, S4A and S10), the increase in TUNEL-positive nuclei (Fig. 4B; Suppl. Fig. S3B and S4B) and the cytosol retraction (Fig. 4C; Suppl. Figs. S3C and S4C).

In the H_2O_2-treated cells, the addition of carnosine and hydralazine greatly suppressed the carbonyl levels (Fig. 3B). Carnosine effectively prevented the H_2O_2-induced growth inhibition and the death of BY-2 cells (Fig. 1A-i). Hydralazine also suppressed the cell death, although the compound itself showed weak cytotoxicity (Fig. 1A-ii). As expected, all of the PCD-associated events caused by H_2O_2 were strongly suppressed by carnosine and hydralazine; i.e., the DNA laddering (Fig. 2A), the increase in TUNEL-positive nuclei (Fig. 2B) and the cytosol retraction (Fig. 2D). It appears that hydralazine had a weaker effect on PCD markers, but this was probably due to the low dose of hydralazine used here. Because it showed a toxicity on the growth of the cells (Fig. 1A-ii), we did not add it at a higher concentration. At the concentration we used, hydralazine might have been depleted below optimal scavenger levels by the carbonyls that were continuously produced following the addition of H_2O_2.

These pharmacological results suggested that the H_2O_2-induced PCD was prevented by the scavenging of oxylipin carbonyls. There is, however, a possibility that these scavengers also suppressed ROS because carnosine and hydralazine have been reported to the antioxidant capacities (Aruoma et al., 1989; Daiber et al., 2005). We investigated possibility that these compounds suppressed ROS and LOOH, in the following four ways. First, to examine the direct scavenging of H_2O_2 by these compounds, we incubated H_2O_2 at 5 mM with either carnosine at 5 mM or hydralazine at 1 mM in 50 mM phosphate buffer (pH 7.4) and 0.5 mM

diethylenetriaminepentaacetic acid at 25°C. After a 30-min incubation, we found no significant decrease in the H_2O_2 amount as determined by the catalase-mediated O_2 evolution (data not shown). Thus, these carbonyl scavengers do not significantly scavenge H_2O_2 at the concentrations we used.

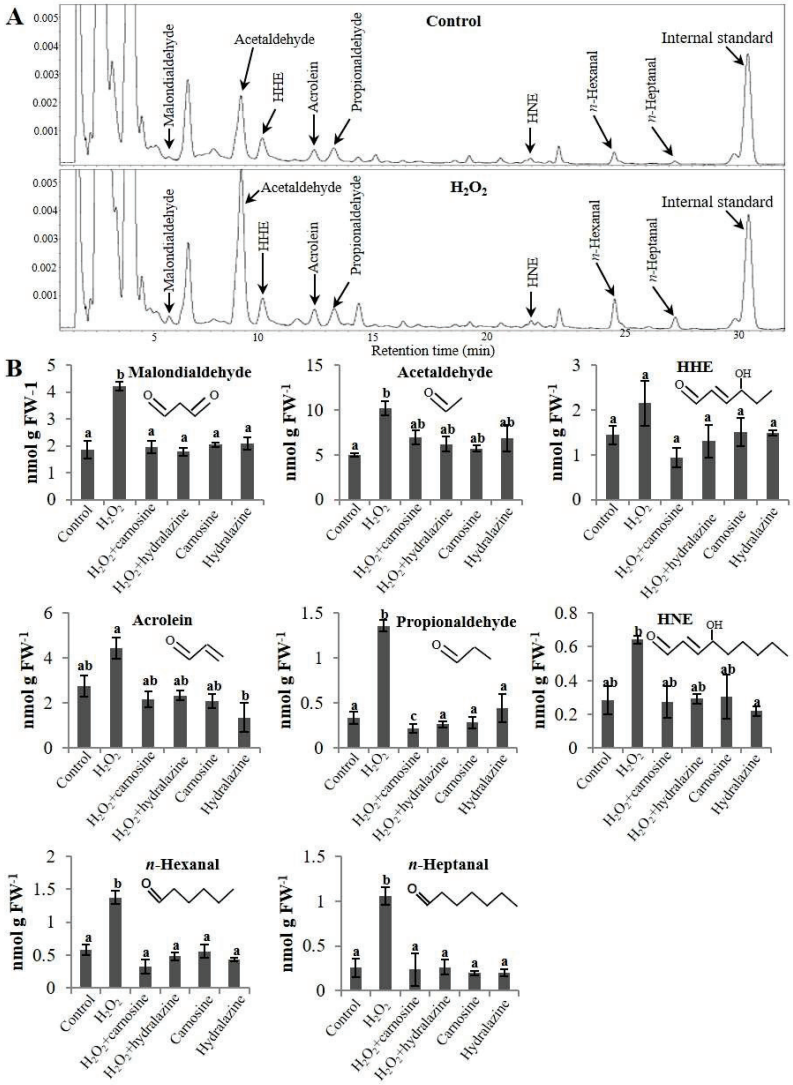

Fig. 3. Effects of H_2O_2 and carbonyl scavengers on the carbonyl contents in BY-2 cells. Four-day-cultured cells were treated with water as control, 1 mM H_2O_2, and 1 mM H_2O_2 plus 2 mM carnosine or 0.2 mM hydralazine for 2 h. Carbonyls were extracted from them, derivatized with 2,4-dinitrophenylhydrazine and separated on HPLC as described in the Materials and Methods. (A) Typical chromatograms showing the carbonyls in the control (upper) and H_2O_2-treated BY-2 cells (lower). The identified aldehydes are labeled at the top of each peak. (B) The intracellular contents of malondialdehyde, acetaldehyde, HHE, acrolein, propionaldehyde, HNE, *n*-hexanal, and *n*-heptanal. Mean ± SEM of three independent experiments. Differences among treatments were analyzed by Tukey test. $P<0.05$.

Second, we examined the effects of these compounds on the intracellular H_2O_2 level by using BES-H_2O_2-Ac, a highly specific H_2O_2 indicator (Maeda, 2008) (Suppl. Fig. S5). At 2 h after the addition of H_2O_2 to BY-2 cells, the BES-H_2O_2 fluorescence level was lower. The decrease in H_2O_2 was probably due to the induction of H_2O_2-scavenging enzymes such as peroxidases (Tsukagoshi et al., 2010; Xu et al., 2011). In both H_2O_2-stimulated and untreated cells, carnosine and hydralazine, at the concentrations we used, did not affect the intracellular H_2O_2 level.

In the third experiment, we determined the intracellular level of a broader range of ROS by monitoring the oxidation of 2′,7′-dihydrodichlorofluoresein (H_2DCF) (Fig. 5). H_2DCF, formed from the exogenously added H_2DCF-diacetate via enzymatic hydrolysis in the cell, is oxidized by hydroxyl radical, organic peroxyl radicals and reactive nitrogen species $NO^{\bullet}$ and $ONOO^-$ to form the fluorescent dye dichlorofluorescein (DCF). This dye is used for determinations of the formation of general reactive species rather than specific ROS (Halliwell and Gutteridge, 2007).

Untreated control cells showed weak fluorescence, representing the basal level of constitutively formed ROS. When H_2O_2 was added to the cells, the fluorescence level was increased slightly at 30 min, and at 2 h, it became fourfold stronger than that in the untreated control cells (Fig. 5B). The fluorescence had become weaker at 5 h (data not shown). This indicated that the intracellular ROS level was transiently increased by the H_2O_2 stimulus. It should be noted that the changes in DCF fluorescence and BES-H_2O_2 fluorescence after H_2O_2 treatment were apparently different. While the H_2O_2 level was suppressed in stressed cells, the general ROS level was increased. Thus, in the H_2O_2-treated BY-2 cells, DCF fluorescence represented not only the level of H_2O_2, but also the levels of a broader range of ROS. Carnosine and hydralazine did not affect the intracellular ROS levels before or after the H_2O_2 treatment (Fig. 5B), providing evidence that these reagents did not scavenge ROS efficiently in the BY-2 cells.

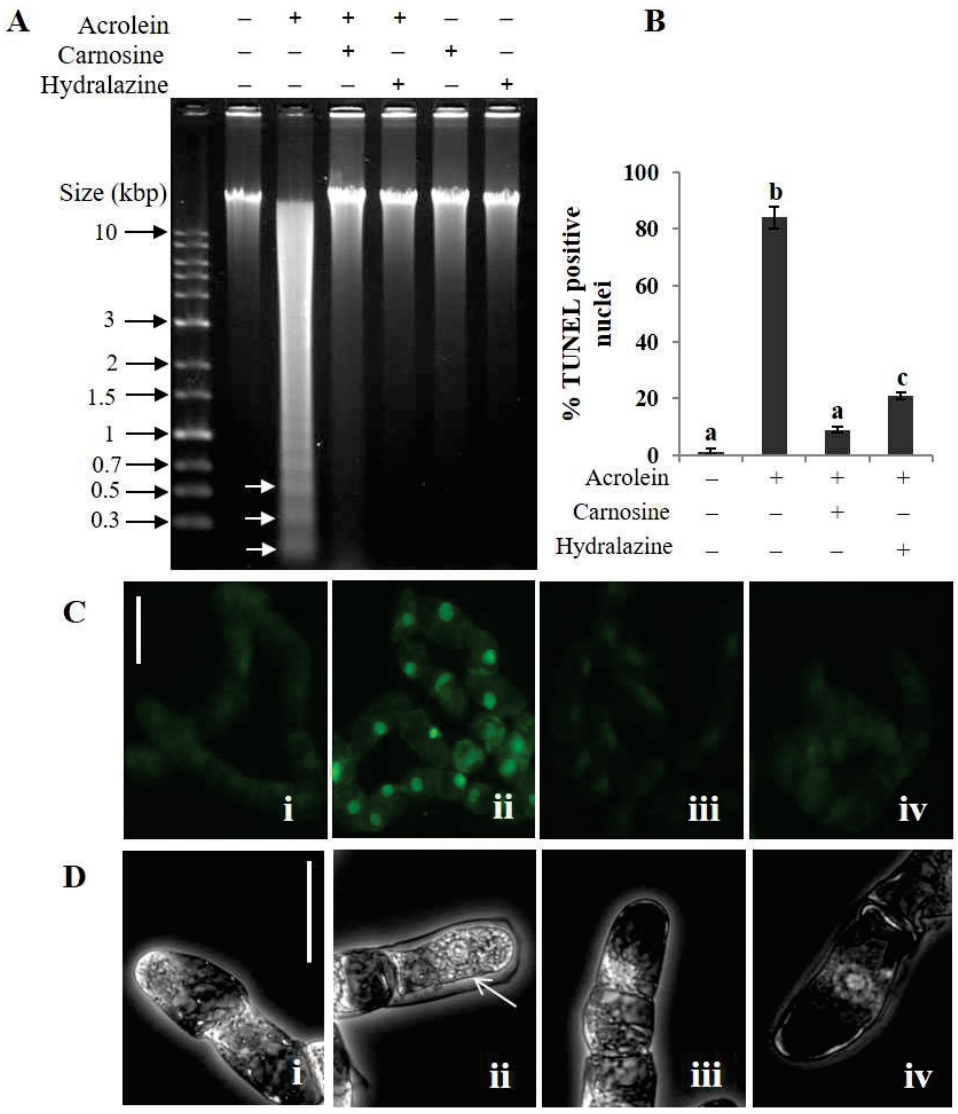

Fig. 4. Induction of PCD in BY-2 cells by acrolein. Four-d-cultured cells were treated with 0.2 mM acrolein or a carbonyl scavenger (1 mM carnosine or 0.2 mM hydralazine) or both as indicated. After 20-h incubation, the cells were used for genomic DNA extraction, the TUNEL assay and cytoplasm retraction observation as described in Materials and Methods. (A) Agarose gel electrophoresis of genomic DNA. White arrows indicate the DNA fragments of 0.18, 0.36 and 0.54 kbp. (B) Fraction of the cells with TUNEL-positive nuclei. The total cell number and the TUNEL-positive cells were counted as in Fig. 2B. Mean ± SEM of three independent experiments. Differences among treatments were analyzed by Tukey test. $P<0.05$. (C) Typical fluorescence microscopy images of the TUNEL assay results: (i) untreated cells as blank control, (ii) 0.2 mM acrolein, (iii) 0.2 mM acrolein + 1 mM carnosine, and (iv) 0.2 mM acrolein + 0.2 mM hydralazine. Bar, 50 µm. (D) Typical phase contrast microscopy images of cell morphology for cytoplasm retraction: (i) untreated control cells, (ii) 0.2 mM acrolein, (iii) 0.2 mM acrolein + 1 mM carnosine, and (iv) 0.2 acrolein mM + 0.2 mM hydralazine. The white arrow in panel (ii) indicates cytosolic retraction. Bar, 50 µm.

In the fourth experiment, we examined the effects of carnosine and hydralazine on the LOOH level. LOOH are products of ROS, and the immediate precursors of oxylipin carbonyls. If the LOOH level is not affected by carnosine or hydralazine, then the observed suppression of carbonyls by these compounds can be explained primarily as a direct scavenging of carbonyls. We determined the LOOH level with the fluorescent probe Spy-LHP (Soh et al., 2007). Spy-LHP, a derivative of diphenyl-1-pyrenylphosphine, has a bulky hydrophobic tail and reacts very rapidly with LOOH to form its oxidized product, Spy-LHPOx, which fluoresces intensely. The reactions of Spy-LHP with $O_2^{-\bullet}$, alkyl hydroperoxyl radical, nitric oxide, and peroxinitrite are insignificant (Soh et al., 2007). Its reaction with H_2O_2 is very slow and can be distinguished from that with LOOH by the measurement of fluorescence increase kinetics (Khorobrykh et al., 2011).

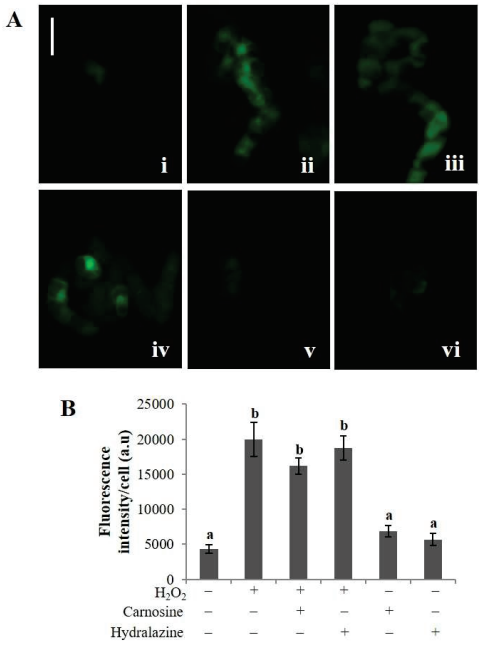

Fig. 5. Carnosine and hydralazine did not affect the increases in the ROS level in BY-2 cells after H_2O_2 treatment. (A) Four-d-cultured cells were incubated with either 1 mM H_2O_2 or a carbonyl scavenger (1 mM carnosine or 0.2 mM hydralazine) or both for 2 h. DCF fluorescence was recorded under a fluorescence microscope as in Materials and Methods. Typical photographs are shown: (i) untreated cells as control, (ii) 1 mM H_2O_2, (iii) 1 mM H_2O_2 + 1 mM carnosine, (iv) 1 mM H_2O_2 + 0.2 mM hydralazine, (v) 1 mM carnosine and (vi) 0.2 mM hydralazine. Bar, 50 µm. (B) The DCF fluorescence intensity of cells. The fluorescence intensity was integrated per cell with ImageJ software. A total of 200 cells were counted in each treatment. Mean of 3 runs ± SEM. Differences among treatments were analyzed by Tukey test. $P<0.05$.

We found that the addition of H_2O_2 to BY-2 cells increased the LOOH level fourfold in 30 min, and it remained high up to 2 h. Neither carnosine nor hydralazine significantly affected the LOOH level (Fig. 6). Thus, under our experimental conditions, carnosine and hydralazine primarily acted as carbonyl scavengers rather than ROS scavengers. The suppression of H_2O_2-induced PCD by these scavengers suggests that the carbonyl species formed in stressed cells participated in the initiation of PCD.

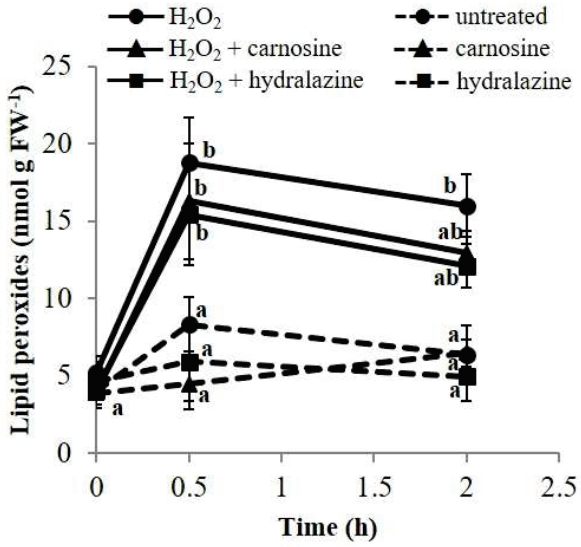

Fig. 6. The carbonyl scavengers carnosine and hydralazine did not suppress LOOH level in BY-2 cells. Four-d-cultured cells were incubated with either 1 mM H_2O_2 or a carbonyl scavenger (1 mM carnosine or 0.2 mM hydralazine) or both for the indicated length. The LOOH level was detected as in Materials and Methods. Mean ± SEM of the data represent three independent experiments. Differences among treatments at the same time point were analyzed by Tukey test. $P<0.05$.

2.3.3 Involvement of oxylipin carbonyls in root PCD

We then examined whether oxylipin carbonyls are involved in PCD in *planta* by combining the pharmacological approach described above with a genetic approach. The addition of H_2O_2 or NaCl to roots causes PCD in the epidermal cells (Demidchik et al., 2010). *A. thaliana* plants grown on an agar plate for 6 d were stressed with 0.2 mM H_2O_2 (Suppl. Fig. S6A-ii and B) or 150 mM NaCl (Suppl. Fig. S7A-ii and B) for 20 h. Both the H_2O_2- and NaCl

treatments resulted in approx. 60 TUNEL-positive cells per half mm of root apex. The protoplast retraction in root hairs and the concomitant loss of the FDA-fluorescing ability in the roots treated with H_2O_2 (Suppl. Fig. S6C-ii) or NaCl (Suppl. Fig. S7C-ii) also indicated the occurrence of PCD (Hogg et al., 2011; Reape and McCabe, 2008).

When carnosine (3 mM) or hydralazine (0.2 mM) was supplemented in the medium, all of the PCD-associated events caused by H_2O_2 and NaCl were largely suppressed. Specifically, the number of TUNEL-positive nuclei was decreased (Suppl. Figs. S6 and S7A-iii, iv) and protoplast retraction in root hairs was prevented (Suppl. Figs. S6 and S7C-iii, iv).

Carbonyl scavengers suppressed oxylipin carbonyls but did not affect the intracellular levels of H_2O_2 in the root tissues: In *A. thaliana* plants exposed to 150 mM NaCl for 20 h, an accumulation of carbonyls along the vascular cylinder was observed as a pink color development of Schiff's reagent (Suppl. Fig. S8-ii). When carnosine or hydralazine was added to the plants concomitantly with NaCl, the color developed only weakly (Suppl. Fig. S8-iii, iv). These carbonyl scavengers also did not affect the BES-H_2O_2 fluorescence level in H_2O_2-treated root apex (Suppl. Fig. S9). Thus oxylipin carbonyls appeared to be involved in *in planta* PCD as well.

To obtain genetic evidence for the involvement of oxylipin carbonyls in PCD, we used transgenic tobacco (*Nicotiana tabacum*) plants overexpressing *A. thaliana* AER (Mano et al., 2005). AER catalyzes the NADPH-dependent reduction of the α,β-unsaturated bond in 2-alkenals such as HNE (Mano et al., 2002). The AER-overexpressing tobaccos accumulate smaller amounts of carbonyls upon oxidative stress than does the wild type SR1 (Mano et al., 2010; Yin et al., 2010).

In the present study, SR1 and the AER-overexpressing line P1#18 plants grown on agar plates were exposed to H_2O_2 or NaCl. Treatment with 2 mM H_2O_2 and 175 mM NaCl for 20 h

respectively resulted in approx. 50 and 40 TUNEL-positive nuclei per 1 mm of root apex in SR1 plants, whereas in the P1#18 plants both treatments produced only approx. 10 TUNEL-positive nuclei (Fig. 7B). Most of the root hair cells in the SR1 plants exposed to H_2O_2 and NaCl showed protoplast retraction and lost the ability to exhibit FDA fluorescence, whereas the root hair cells in the P1#18 plants showed much fewer PCD symptoms (Fig. 8).

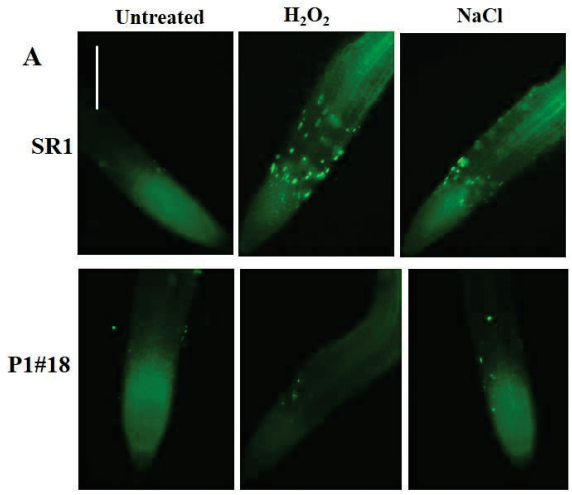

B

Line	Number of TUNEL positive nuclei / mm root tip		
	Control	H_2O_2	NaCl
SR1	9.0 ± 1.2	56.7 ± 9.7	37.3 ± 5.2
P1#18	10.0 ± 1.7	14.3 ± 2.0	23.0 ± 1.7
difference	n.s.	P <0.05	P <0.05

Fig. 7. PCD in the roots of wild type tobacco SR1 line and the AER-overexpression line P1#18. Six-d-old plants were transferred to fresh MS medium supplemented with either 2 mM H_2O_2 or 175 mM NaCl. After a 20-h incubation, root tips of about 5 mm length were excised from the plant and used for TUNEL assay as described in Materials and Methods. (A) Typical fluorescence images for TUNEL assay. Bar, 250 μm. (B) Fraction of the cells with TUNEL-positive nuclei. TUNEL positive cells were counted in 1 mm from the tip of primary root. A total of 9 roots were counted in each treatment. The difference between the lines was examined by Student's *t*-test. "n.s.", not significant.

The overexpression of AER did not affect the intracellular ROS level (Fig. 9). The DCF fluorescence level was low under non-stressed conditions, and it was increased by the treatment with H_2O_2 and NaCl, especially at the elongation zone in the root apex. The SR1 and P1#18 plants showed the same fluorescence level before the stress treatments and after

the treatments. Specifically, the lowered PCD rate in the AER-overexpression plants was ascribed to the scavenging of carbonyls by AER. These pharmacological and genetic results indicate the direct contribution of oxylipin carbonyls to PCD in the H_2O_2- and NaCl-stressed roots.

2.3.4 Strength of each carbonyl to cause PCD

The α,β-unsaturated aldehydes such as HNE and acrolein are highly electrophilic and generally highly reactive, whereas saturated aldehydes such as *n*-hexanal and propionaldehyde are less reactive. To obtain insights into the roles of individual carbonyls that are formed in stressed plant cells, we evaluated the PCD-inducing strength of these carbonyls. We defined the strength of a carbonyl species as the lowest concentration of it

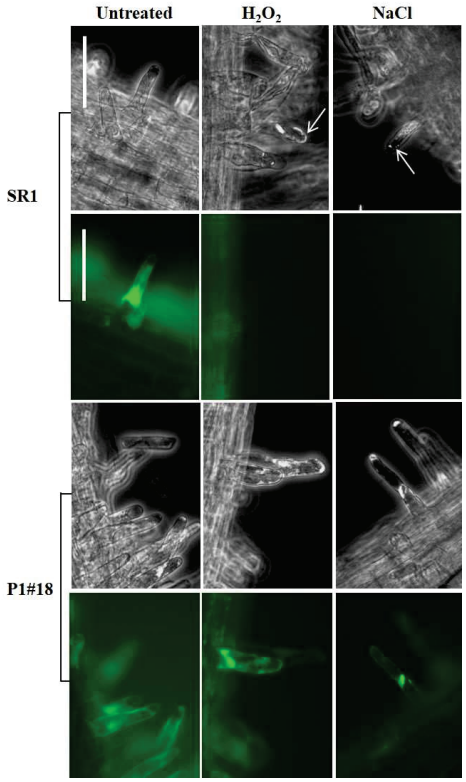

Fig. 8. Root hair PCD in the wild type tobacco SR1 line and the AER-overexpression P1#18 line. Six-d-old plants were treated with H_2O_2 or NaCl as in Fig. 7. After a 20-h incubation, root tips of 5 mm length were excised and used for FDA staining as described in Materials and Methods. Typical phase contrast images for cytoplasm retraction (upper row for each line) and fluorescence images of the same field (lower row). White arrowhead indicates cytoplasm retraction. Bar, 100 μm.

that would cause DNA laddering in tobacco BY-2 cells (Table 1, Suppl. Figs. S4 and S10). As expected, the strongest carbonyls were acrolein and HNE. These caused the DNA laddering, TUNEL-positive nuclei and cytoplasm retraction (Fig. 4, Suppl. Fig. S3) at concentrations as low as 0.2 mM. The next-strongest carbonyls were *n*-hexanal, *n*-heptanal and (*Z*)-3-hexenal (3 mM required for PCD) and the weakest was propionaldehyde (50 mM).

We also tested the PCD-inducing ability of carbonyls *in planta* and found that acrolein and HNE at 1 mM and propionaldyde at 10 mM effectively developed PCD markers in root hairs of *A. thaliana* such as protoplast retraction and a concomitant loss of the FDA-fluorescing ability (Suppl. Fig. S11). Thus, the PCD-inducing strength of carbonyls differs by species, but most species of oxylipin carbonyls that were generated in H_2O_2-stressed cells (Fig. 3) can cause PCD.

2.4. Discussion

2.4.1 Oxylipin carbonyls can mediate H_2O_2- and NaCl-induced PCD

We investigated the roles of oxylipin carbonyls in plant injury under oxidative stress. As experimental models, we used H_2O_2-induced damage to tobacco BY-2 cells and H_2O_2- and NaCl-induced damage to roots of tobacco and *A. thaliana*. In these experiments, we found that the stress treatment commonly induced PCD, and that the scavenging of endogenous oxylipin carbonyls with chemical scavengers or a specific enzyme blocked the PCD. We identified the oxylipin carbonyl species that were increased in H_2O_2-treated BY-2 cells. These species when added exogenously could induce PCD in BY-2 cells and roots. From these results, we concluded that oxylipin carbonyls, downstream products of ROS, significantly contributed to the initiation of PCD in H_2O_2- or NaCl-stressed cells.

The involvement of oxylipin carbonyls in plant PCD shown in this study may not be

surprising. For animal cells, it is established that reactive oxylipin carbonyls such as HNE have the potential to cause apoptosis, and their involvement in oxidative signal-induced PCD has been studied extensively (reviewed by Dalleau et al., 2013). For plant cells, the toxicity of oxylipin carbonyls has been recognized recently, but their ability to produce cellular damage has not been investigated. An achievement in our present study was that we identified the carbonyl species that are generated and can cause PCD in stressed cells. In addition, our findings demonstrated that not only ROS but also oxylipin carbonyls were necessary for the development of PCD under H_2O_2 and NaCl stress. Specifically, these oxylipin carbonyls were the chemical entities that initiated plant PCD. Although such critical involvement of oxylipin carbonyls may be valid only for certain types of stress, the present results provide a new clue to understanding the toxicity of ROS in plant cells.

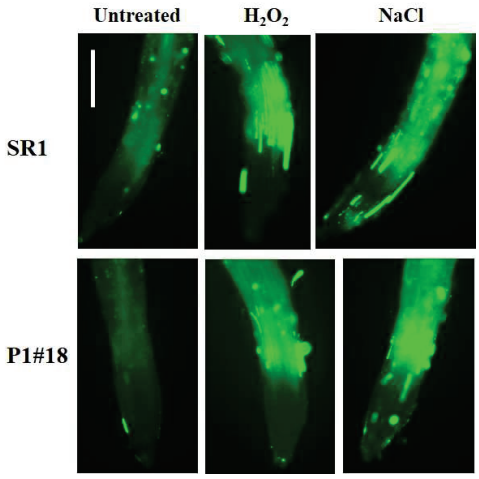

Fig. 9. Distribution of ROS in the root of wild type tobacco SR1 line and the AER-overexpression P1#18 line. Six-d-old plants were treated with H_2O_2 or NaCl as in Fig. 7. After a 20-h incubation, root tips of 5 mm length were excised from the primary root. DCF fluorescence was recorded as in Materials and Methods. Typical images of DCF fluorescence are shown. Bar, 250 µm.

2.4.2 Multiple species of oxylipin carbonyls appear to contribute to PCD

The oxylipin carbonyls identified in the H_2O_2-stressed cells included the α,β-unsaturated carbonyls acrolein and HNE, and the saturated carbonyls *n*-hexenal, *n*-heptanal and propionaldehyde, and (*Z*)-3-hexenal. All carbonyls can modify proteins via Schiff-base

formation with an amino group. The α,β-unsaturated carbonyls are known to have higher cytotoxicity than other types of carbonyls because they are strong electrophiles and can form Michael-adducts with the Cys, His and Lys residues in addition to the Schiff base. Indeed, HNE and acrolein induced PCD in BY-2 cells at 0.3 mM. What we did not expect was that saturated carbonyls such as *n*-hexanal and *n*-heptanal also have the ability to initiate PCD. The strength order of these carbonyls to induce PCD corresponded with the order of chemical reactivity (Table 1).

Considering that *n*-hexenal and *n*-heptanal were more greatly increased than acrolein and HNE in the H_2O_2-stimulated cells, we suggest the possibility that these saturated carbonyls also substantially contributed to the induction of PCD in the stressed cells. The inhibition of PCD by the overexpression of AER does not exclude the involvement of saturated carbonyls because in the AER-overproducing plants, the scavenging of the α,β-unsaturated carbonyls resulted in the suppression of the stress-induced increase in saturated carbonyls, probably as a secondary effect (Yin et al., 2010). These two types of carbonyls might mediate PCD by different mechanisms, i.e., via different receptors/sensors (discussed below). It is necessary to investigate the effect of distinct carbonyls on different pathways.

In addition, the finding that various carbonyls have the capacity to induce PCD may explain the diversity and number of carbonyl-scavenging enzymes. There are four classes of carbonyl-scavenging enzymes in plants: aldehyde dehydrogenases (Kirch et al., 2001), aldo-keto reductases (Oberschall et al., 2000), 2-alkenal reductases (Mano et al., 2005) and glutathione *S*-transferases (Gronwald and Plaisance, 1998). In the *A. thaliana* genome, a dozen isozymes or more are encoded for each class. These enzymes in different classes have different substrate specificities, and even in the same class, isozymes show different specificities. There must have been selective pressure on plants to obtain a large set of scavenging enzymes to harness oxylipin carbonyls so that they would not trigger PCD unless it is to be commanded.

2.4.3 Oxylipin carbonyls as mediators of oxidative signals in environmental stress responses

ROS-induced cell death in plants has been demonstrated for various environmental stressors (Mittler et al., 2011; Petrov et al., 2015). In the present study we investigated the cell death induced by H_2O_2 and NaCl. NaCl treatment activates the plasma membrane NADPH oxidases to facilitate superoxide production, from which H_2O_2 is formed via catalysis with superoxide dismutase. NaCl treatment also activates polyamine oxidase, which catalyzes the production of H_2O_2 in the oxidation of spermine and spermidine. Thus NaCl treatment also imposes H_2O_2 stress on plant cells (Petrov et al., 2015). When they were stressed, both cultured cells and root cells showed TUNEL-positive nuclei, cytosolic retraction and DNA laddering, which are typical of apoptosis-like PCD (Reape and McCabe 2008).

Two oxidative signal pathways for PCD are reported; one is the mitochondria-dependent activation of caspase-like proteases as in animal cell apoptosis (Reape and McCabe, 2008), and the other is the mitogen-activated protein kinase (MAPK) cascade (Nakagami et al., 2006). In either case, the receptors or sensors for ROS have been largely elusive (Gadjev et al., 2008). Our finding that the oxylipin carbonyls caused PCD suggests that these compounds participate in the signal pathway, at least in part, as mediators just downstream of ROS.

The PCD-initiating role of oxylipin carbonyls in whole plants may not be restricted to NaCl stress. The overexpression of carbonyl-scavenging enzymes improves plants' tolerance not only to salinity, but also to heavy metals, drought (Sunker et al., 2003), UV-B (Hideg et al., 2003), strong light (Mano et al., 2010) and aluminum (Yin et al., 2010). Among these stressors, UV-B and aluminum are known to cause PCD. Analysis of the mode of cell death and oxylipin carbonyls will clarify the roles of these compounds in PCD induced by the different condtions.

From a broader perspective, ROS-triggered PCD has been observed in a hypersensitive response after pathogen infection (Torres et al., 2005) and certain developmental events such as lateral root cap shedding (Pennell and Lamb, 1997), aleurone layer death during the germination of cereal grains (Bethke and Jones, 2001), the development of tracheary elements in the xylem of vascular plants (Kuriyama and Fukuda, 2002), leaf senescence (Zapata et al., 2005), and the nucellar cell elimination during the endosperm formation in *Sechium edule* (Lombardi et al., 2010). Because the production of oxylipin carbonyls is closely associated with the occurrence of ROS, we can expect their involvement in these physiological responses. The use of carbonyl scavengers such as carnosine or enzymes in combination with the chemical analysis of the involved carbonyls will be a good test to judge the broader physiological aspects of the operation of the carbonyl signal in plant PCD.

2.4.4 How do oxylipin carbonyls initiate PCD?

Because of their high reactivity, the α,β-unsaturated carbonyls such as HNE and acrolein may exert indiscriminate damage to proteins, but they target only limited types of proteins *in vivo*. Winger et al., (2007) analyzed the HNE modification of mitochondrial proteins in *A. thaliana* cells. They identified 16 distinct proteins that were sensitively modified under oxidative stress. In salt-stressed *A. thaliana* leaves, even when the tissue started to die, only 17 protein species showed more than a twofold increase in HNE modification (Mano et al., 2014b). Thus oxylipin carbonyls have chemical specificity required for ROS signaling (Møller and Sweetlove, 2010). In other words, specific receptors/sensors of oxylipin carbonyls may exist. Indeed, the redox-regulated NPR proteins and TGA transcription factors are candidates for the carbonyl sensors (Farmer and Mueller, 2013) but not for PCD induction.

As judged on the morphological change and DNA fragmentation, the H_2O_2- and NaCl-induced PCD in the present study was of the apoptosis-like mode, in which a

mitochondria-dependent activation of proteases (caspase-like proteases) is involved (Reape and McCabe, 2008). In the mitochondria-dependent apoptosis in animal cells, several proteins are suggested as HNE targets, such as the Fas protein and the tumor suppressor/cell cycle regulator protein p53 (Dalleau et al., 2013), but plant cells do not have proteins apparently homologous to these HNE targets. The primary effect of HNE on plant mitochondria might be the inactivation of sensitive target enzymes such as pyruvate dehydrogenase complex and glycine decarboxylase complex (Taylor et al., 2002). A rapid consumption of glutathione via the Michael adduct formation with the α,β-unsaturated carbonyls (Esterbauer et al., 1991) would also affect the redox status of mitochondria. These changes would facilitate the deterioration of the mitochondrial membranes and the formation of pores on the outer membrane to allow the release of mitochondrial PCD-associated proteins.

On the other hand, in the H_2O_2-inducible PCD in *A. thaliana*, a signal transduction mechanism via the regulation of proteasomal degradation is known to be involved in the mitogen-activated protein kinase (MAPK) cascade. Specifically, the protein kinase kinase kinase MEKK1, the most upstream factor of the H_2O_2-induced AtMPK3 and AtMPK6-dependent PCD pathway, is regulated in a proteasome-dependent manner (Nakagami et al., 2006). It was reported in a study of mammalian cells that oxylipin carbonyls are involved in the proteasome-dependent signal regulation via the carbonyl sensor Keap1 (Higdon et al., 2012). In the relaxed state of the cells, Keap1 binds the transcription factor Nrf2, and this binding facilitates the ubiquitination and the subsequent proteasome-dependent degradation of Nrf2, so as to repress the Nrf2-dependent gene expression. HNE formed under oxidative stress modifies Keap1 on the Cys151 residue. The modified Keap1 no longer binds Nrf2, which then escapes from ubiquitination. Thus Keap1 receives and transduces the carbonyl signal via the attenuation of the proteasome-dependent degradation of Nrf2 to induce defense responses (Higdon et al., 2012). It is unclear how H_2O_2 suppresses the proteasome-dependent MEKK1 degradation, but it is likely that the MEKK1 degradation is

regulated by a protein that is functionally similar to Keap1. Oxylipin carbonyls may act on such a regulator.

We recently identified 17 species of proteins that are sensitively modified with HNE in the leaves of *A. thaliana* under salt stress (Mano et al., 2014b). Among them, several proteins are candidates to determine cell fate, as follows. One is the chloroplastic peptidyl-prolyl *cis-trans* isomerase (also named cyclophilin 20-3), which plays a key role in cysteine biosynthesis. The modification of its redox active Cys residues with 12-oxo-phytodienoic acid, a long-chain oxylipin carbonyl, triggers the formation of cysteine synthase complex, thereby activating sulfur assimilation and building up cellular redox potential (Park et al., 2013). Modification of these carbonyl-prone Cys residues with short-chain oxylipin carbonyls might have different effects on the protein's function.

Another candidate is nitrilase 1 (Nit1), a highly conserved protein that functions as a tumor suppressor (Sun et al., 2009). In *A. thaliana*, changes in the polymer structure and the intracellular localization of Nit1 are closely associated with the transition from proliferation to differentiation (Doskočilová et al., 2013). It is, however, unclear whether the HNE modification of Nit1 causes such changes. We are now investigating the effects of the carbonyl modification of each target protein on cell fate.

2.5 Materials and Methods

2.5.1 Culture of cells and plants

The suspension of tobacco BY-2 cells (*Nicotiana tabacum* L. cv. Bright Yellow-2) was cultured in Murashige & Skoog (MS) medium supplemented with sucrose (30 g L^{-1}), myo-inositol (100 mg L^{-1}), KH_2PO_4 (200 mg L^{-1}), thiamine HCl (0.5 mg L^{-1}) and 2,4-dichlorophenoxyacetic acid (0.2 mg L^{-1}), pH 5.6. The cells were cultured in darkness at 25°C with continuous rotation at 120 rpm. Every 7 days, 50 mg of cells were transferred to a

flask of 50 mL of fresh medium. Four-day culture cells were used for PCD treatment. In this exponential growth phase, cells remain in the maximum mitotic stage (Nagata et al., 2004). Cells were collected by filtration and washed once with distilled water for analysis.

Wild-type tobacco (*N. tabacum* L. cv. Petit Havana SR1), the transgenic line P1#18 that overexpresses *A. thaliana* alkenal reductase (AER) (Mano et al., 2005) and *A. thaliana* ecotype Columbia-0 were grown vertically on 1% agar plates (half-strength MS medium), in sterile condition, at 23°C in a 14-h light/10-h dark cycle (light intensity, 100 μmol m^{-2} s^{-1} with white fluorescence lamps).

2.5.2 Trypan-blue staining for cell death

A 0.2-mL aliquot of cell suspension was added to a mixture of 0.3 mL of 3% sucrose and 0.5 mL of 4% trypan blue solution. After 10 min, cells were washed once with phosphate-buffered saline (PBS), and then 10 μL of the cell suspension was transferred to a microscopic slide and the dead (trypan blue-stained) and live (unstained) cells were counted. Cell death is expressed as the percentage of dead cells.

2.5.3 Isolation of genomic DNA and gel electrophoresis

Approximately 200 mg of BY-2 cells were ground with a mortar and pestle that were chilled with liquid nitrogen. The resulting powder was transferred to a 1.5-mL microtube, and 0.7 mL of extraction buffer containing 2% cetyltrimethylammonium bromide, 1.4 M NaCl, 20 mM EDTA, 100 mM Tris-HCl, pH 8.0 and 0.2% β-mercapto-ethanol was added immediately. The mixture was incubated at 65°C for 45 min. After centrifugation at 12,000 × *g* for 15 min at room temperature, the supernatant was treated with RNase A (10 mg mL^{-1}) at 37°C for 1 h and then mixed well with an equal volume of the chloroform:isoamyl alcohol mixture (24:1). After centrifugation at 10,000 × *g* for 12 min, the upper aqueous phase was collected. The DNA was precipitated with a two-thirds volume of isopropanol, washed in 70% ethanol, dried,

and resuspended in sterile distilled water. The DNA was then electrophoresed on a 1% agarose gel followed by visualization with ethidium bromide.

2.5.4 Detection of nuclear DNA fragmentation using a TUNEL assay

We used the *In Situ* Cell Death Detection kit: Fluorescence (Roche Diagnostics, Mannheim, Germany) to determine cell death, according to the manufacturer's instructions with minor modification. Four-d culture cells were treated for 20 h with H_2O_2 or acrolein plus scavengers and then harvested for staining. The cells were fixed with 4% (v/v) fresh paraformaldehyde in PBS and labeled by the TUNEL reaction mixture: the terminal deoxynuleotidyl transferase solution and the label solution described in the kit's manual. The transferase was omitted for the negative control. For the positive control, we incubated fixed and permeabilized cells with DNase I to induce DNA strand breaks prior to the TUNEL reaction. The technique was adjusted for the study of the whole root and observation of the epidermal cells. Roots were permeabilized for 20 min in a solution containing 0.1% Triton-X, 0.1% sodium citrate, 0.1 mM KCl and 0.1 mM $CaCl_2$. The stained cells and roots were analyzed under a fluorescence microscope (Leica AF6000, Wetzlar, Germany). The excitation and emission wavelengths were 488 nm and 515 nm, respectively.

2.5.5 Detection and quantification of carbonyls using HPLC

Freshly harvested cells (0.45 g) were added to 3 mL acetonitrile containing 60 nmol 2-ethylhexanal (as an internal standard) and 0.005% (w/v) butylhydroxytoluene and then incubated in a screw-capped glass tube at 60°C for 30 min. Carbonyls in the extract were derivatized with 2,4-dinitrophenylhydrazine, and the dinitrophenylhydrazone (DNP) derivatives were extracted and analyzed by high-performance liquid chromatography (HPLC) as described (Yin et al., 2010). We identified DNP derivatives of carbonyls by their retention time and determined their contents by a comparison with authentic compounds (Matsui et al., 2009).

2.5.6 ROS detection with H_2DCF-diacetate and H_2O_2 detection with the BES-H_2O_2-Ac probe

BY-2 cells, collected with a brief centrifugation followed by a washing with distilled water, were incubated in 20 µM H_2DCF-diacetate (Molecular Probes, Eugene, OR, USA) in PBS at 37°C for 30 min or 50 µM BES-H_2O_2-Ac (Wako Pure Chemical, Osaka, Japan) for 30 min in darkness. The cells were washed twice with PBS. For tobacco and *A. thaliana* roots, 5 mm of root apex were excised and incubated in 50 µM H_2DCF-diacetate in 20 mM K-phosphate, pH 6.0, or in 50 µM BES-H_2O_2-Ac in darkness for 30 min and washed two times with PBS. The fluorescence was monitored under a microscope with excitation at 488 nm and emission at 530 nm for both DCF and BES-H_2O_2.

2.5.7 Detection of LOOH with Spy-HP

BY-2 cells were collected via filtration and washed once with distilled water. Then 0.4 g cells were taken in a tube, and 100 µL of suspension medium (50 mM Mes-NaOH, pH 6.5 and 35 mM NaCl) and 2.7 µM Spy-LHP (Dojindo Laboratories, Kumamoto, Japan) in ethanol (900 µL) were added. After a 30-min incubation at 37°C, the samples were centrifuged at 12,000 × *g* for 2 min. The supernatant was collected, and its fluorescence was measured with a spectrofluorometer (FP 8300, JASCO, Hachioji, Japan) with excitation at 524 nm and emission at 538 nm. For determining the amount of peroxides, a standard curve was prepared with a model LOOH *m*-chloroperbenzoic acid (Khorobrykh et al., 2011).

2.5.8 Visualization of the accumulation of carbonyls in roots

Root tips (approx. 2 cm from the tip) were excised and stained with Schiff's reagent (Wako) for 20 min at room temperature, then rinsed with a freshly prepare sulfite solution (0.5% [w/v] $K_2S_2O_2$ in 0.05 M HCl) and kept in the sulfite solution and observed under a light microscope (Leica LED3000).

2.5.9 Root hair PCD assay

Roots were stained with fluorescein diacetate (FDA; Wako) for the detection of PCD. Only viable root hairs are able to cleave FDA to form fluorescein and fluoresce green under a microscope with excitation at 485 nm. Dead cells do not fluoresce, and their protoplasts retract from the cell wall. Roots were stained in a 10-μg mL^{-1} solution of FDA on microscope slides, and root hairs were immediately observed under a fluorescence microscope (Leica AF6000).

2.6 Supplementary data

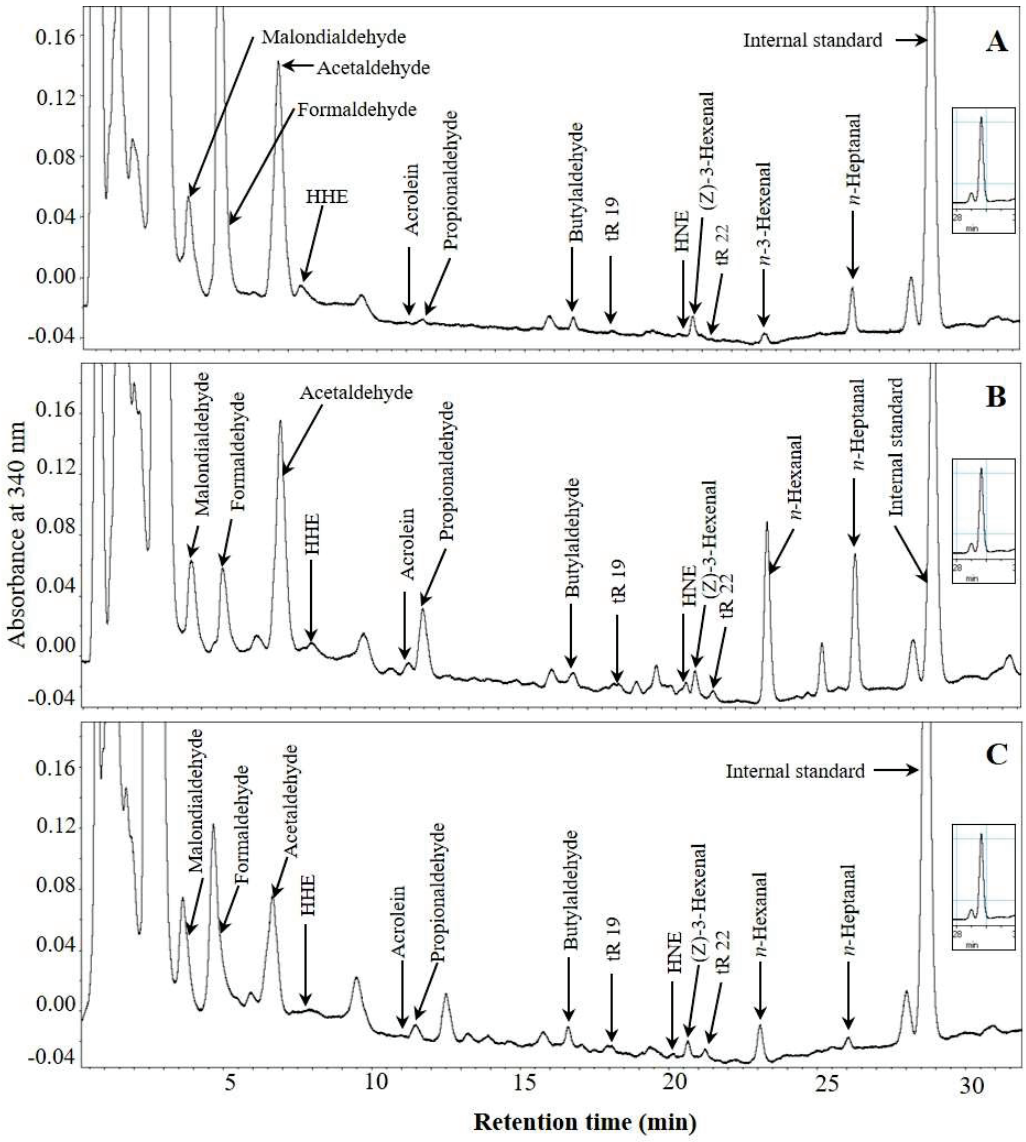

Supplemental Figure S1. Typical chromatograms showing the carbonyls in BY-2 cells (5 h treatment). (A) control, (B) H_2O_2-treated and (C) H_2O_2 plus hydralazine. To four-d-cultured cells 1 mM H_2O_2 and 0.2 mM hydralazine were added. Carbonyls were analyzed on HPLC as in Fig. 2. The identified aldehydes are labelled at the top of each peak. The inset peaks show the internal standard.

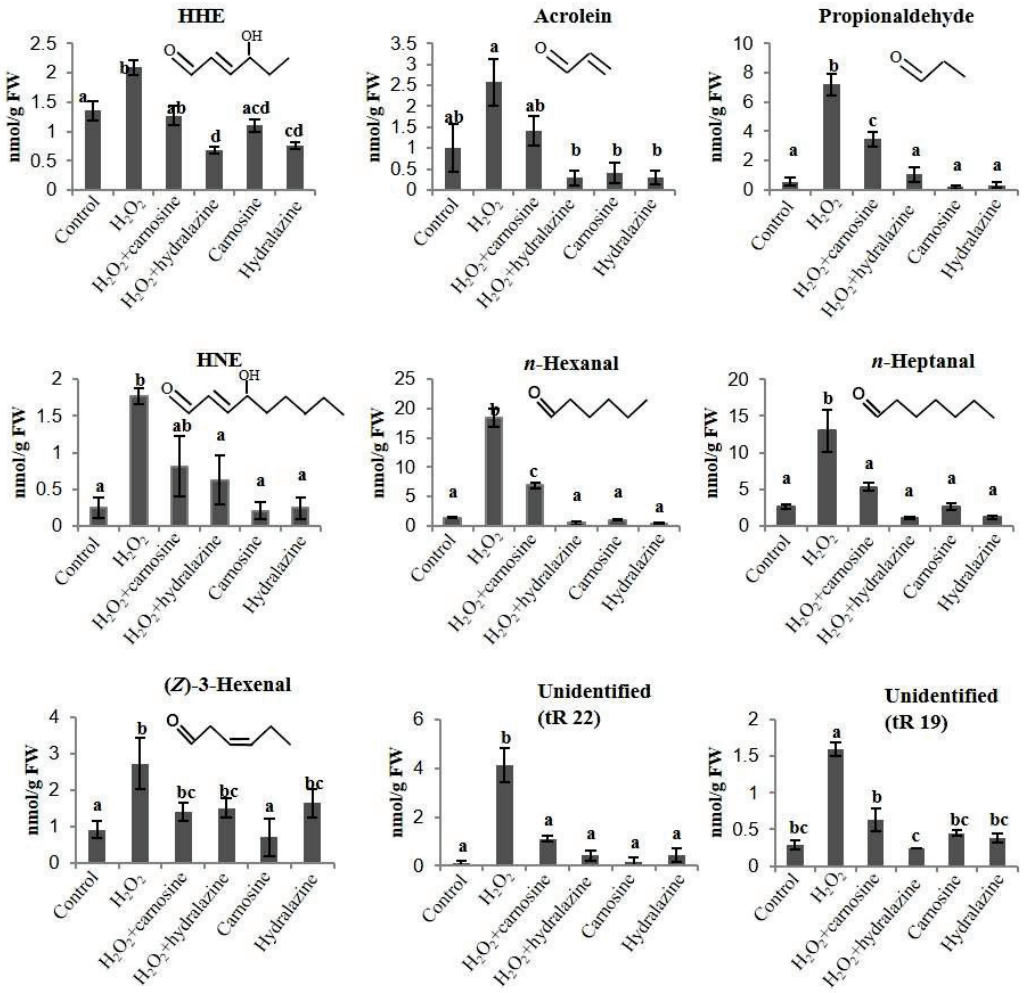

Supplemental Figure S2. Effects of H_2O_2 and RCS scavengers on the carbonyl levels in BY-2 cells (5 h experiment). Four-day-cultured cells were treated with water as control, 1 mM H_2O_2, and 1 mM H_2O_2 plus 1 mM carnosine or 0.2 mM hydralazine for 5 h. The intracellular contents of HHE, acrolein, propionaldehyde, HNE, *n*-hexanal, *n*-heptanal, 3-(*Z*)-hexanal and two unidentified carbonyls tR22 and tR19. Mean ± SEM of three independent experiments. Differences among treatments were analyzed by Tukey test. $P<0.05$.

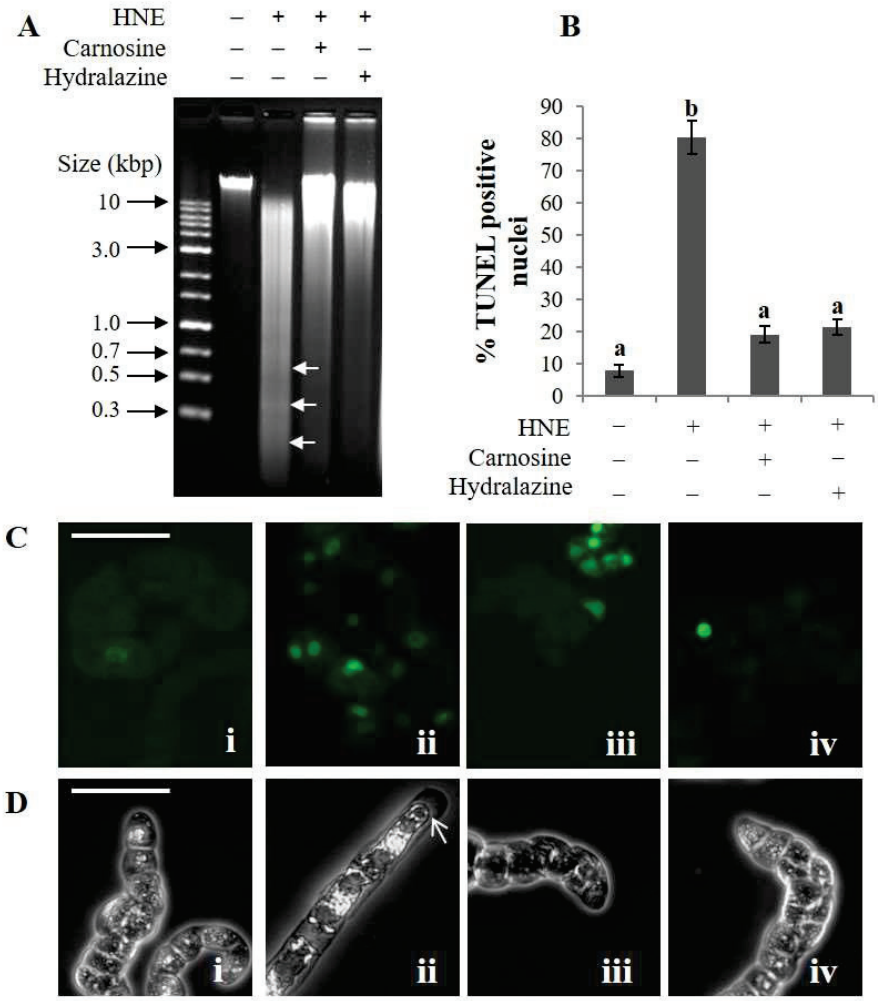

Supplemental Figure S3: Induction of PCD in BY-2 cells by HNE. Four-d-cultured cells were treated with 0.2 mM HNE or a carbonyl scavenger (1 mM carnosine or 0.2 mM hydralazine) or both as indicated. After 20-h incubation, the cells were used for genomic DNA extraction, the TUNEL assay and cytoplasm retraction observation as described in Materials and Methods. (A) Agarose gel electrophoresis of genomic DNA. White arrows indicate the DNA fragments of 0.18, 0.36 and 0.54 kbp. (B) Fraction of the cells with TUNEL-positive nuclei. Cells forming a single layer under microscopy were chosen for the evaluation. The total cell number and the TUNEL-positive cells were counted as in (Fig. 2B). Differences among treatments were analyzed by Tukey test. $P<0.05$. (C) Typical fluorescence microscopy images of the TUNEL assay results: (i) untreated cells as blank control, (ii) 0.2 mM HNE, (iii) 0.2 mM HNE + 1 mM carnosine, and (iv) 0.2 mM HNE + 0.2 mM hydralazine. All values are mean ± SEM, and the data represent three independent experiments. Bar, 50 μm (D) Typical phase contrast microscopy images of cell morphology for cytoplasm retraction: (i)-(iv), same as in (C). The white arrow in the panel (ii) indicates cytosolic retraction.

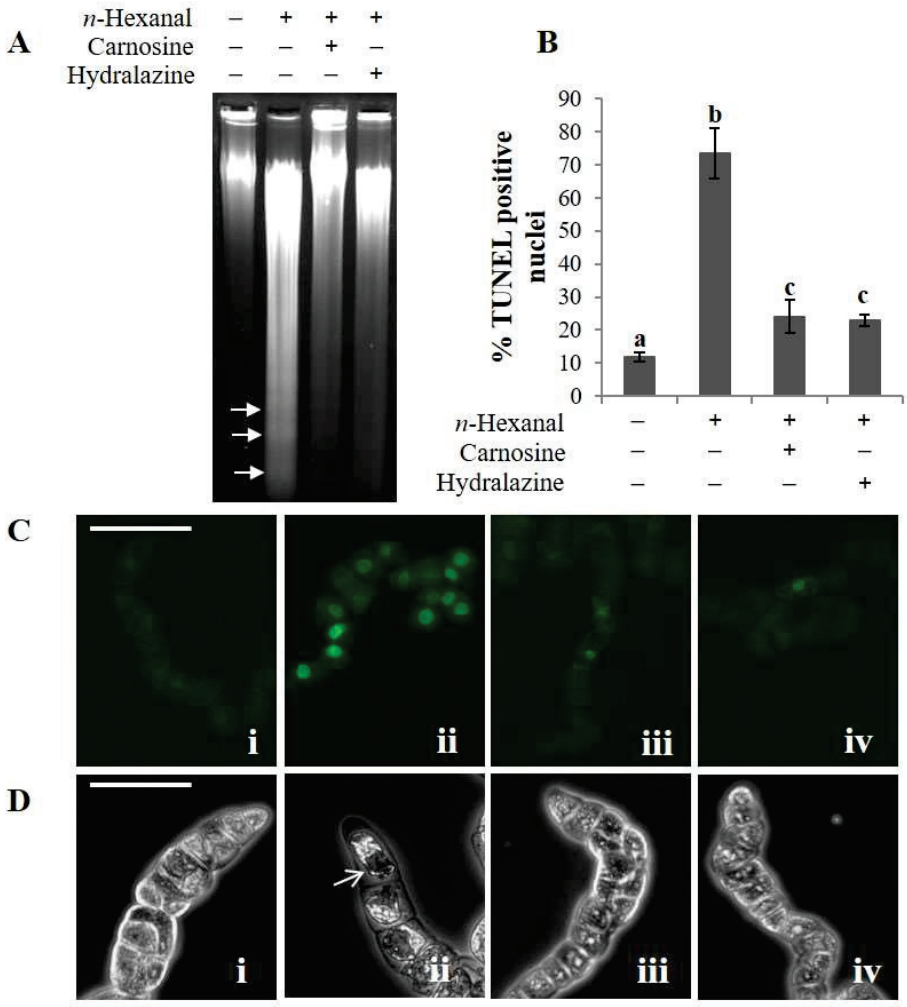

Supplemental Figure S4: Induction of PCD in BY-2 cells by *n*-hexanal. Four-d-cultured cells were treated with 3 mM *n*-hexanal or a carbonyl scavenger (5 mM carnosine or 0.2 mM hydralazine) or both as indicated. After 20-h incubation, the cells were used for genomic DNA extraction, the TUNEL assay and cytoplasm retraction observation as described in Materials and Methods. (A) Agarose gel electrophoresis of genomic DNA. White arrows indicate the DNA fragments of 0.18, 0.36 and 0.54 kbp. (B) Fraction of the cells with TUNEL-positive nuclei. Cells forming a single layer under microscopy were chosen for the evaluation. The total cell number and the TUNEL-positive cells were counted as in Fig. 2B. Mean ± SEM of three independent experiments. Differences among treatments were analyzed by Tukey test. $P<0.05$. (C) Typical fluorescence microscopy images of the TUNEL assay results: (i) untreated cells as blank control, (ii) 3 mM *n*-hexanal, (iii) 3 mM *n*-hexanal + 5 mM carnosine and (iv) 3 mM *n*-hexanal + 0.2 mM hydralazine. (D) Typical phase contrast microscopy images of cell morphology for cytoplasm retraction: (i)-(iv) same as in (C). The white arrowhead in the panel (ii) indicates cytosolic retraction. Bar, 50 μm.

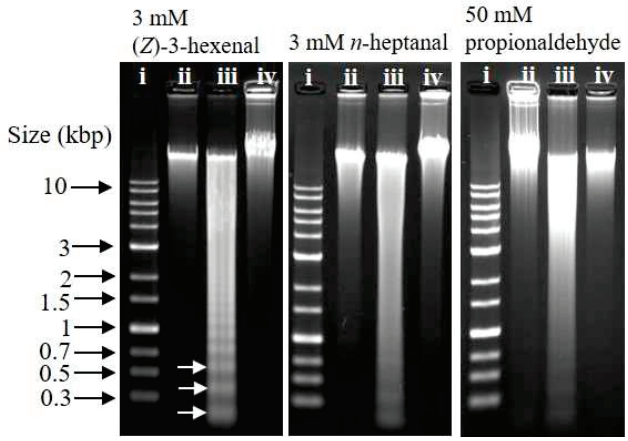

Supplemental Figure S5: DNA fragmentation in the BY-2 cells treated with carbonyls in the absence of H_2O_2. Genomic DNA was extracted from tobacco BY-2 cells 20 h after treatment with the indicated carbonyl. For each panel, lane (i) represents the molecular marker, (ii) untreated cells, (iii) cells treated with the carbonyl only, and (iv) cells treated with carbonyl + carnosine. For each carbonyl, the lowest concentration to induce PCD was used. We added carnosine at the lowest concentration to stop PCD for each carbonyl (3 mM for (*Z*)-3-hexenal, *n*-heptanal and 5 mM for propionaldehyde). White arrowheads indicate the DNA fragments of 0.18, 0.36 and 0.54 kbp.

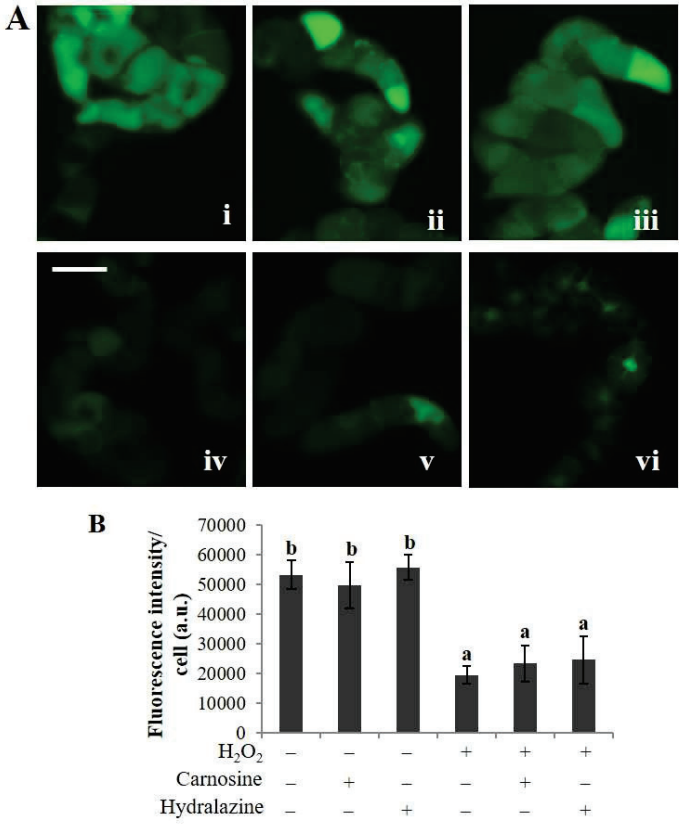

Supplemental Figure S6: Carnosine and hydralazine did not affect the intracellular H_2O_2 level in BY-2 cells. (A) Four-day-cultured cells were incubated with 1 mM H_2O_2 or a carbonyl scavenger (1 mM carnosine or 0.2 mM hydralazine) or both for 2 h. BES-H_2O_2-Ac probe was used to measure the H_2O_2 level as in Materials and Methods. Typical fluorescent microscopy images are shown: (i) untreated cells as control, (ii) 1 mM carnosine, (iii) 0.2 mM hydralazine, (iv) 1 mM H_2O_2, (v) 1 mM H_2O_2 + 1 mM carnosine and (vi) 1 mM H_2O_2 + 0.2 mM hydralazine. Bar, 50 µm. (B) The BES-H_2O_2-fluorescence intensity of cells. The fluorescence intensity was integrated per cell with ImageJ software. A total of 250 cells were counted in each treatment. Mean of 3 runs ± SEM. Differences among treatments were analyzed by Tukey test. $P<0.05$.

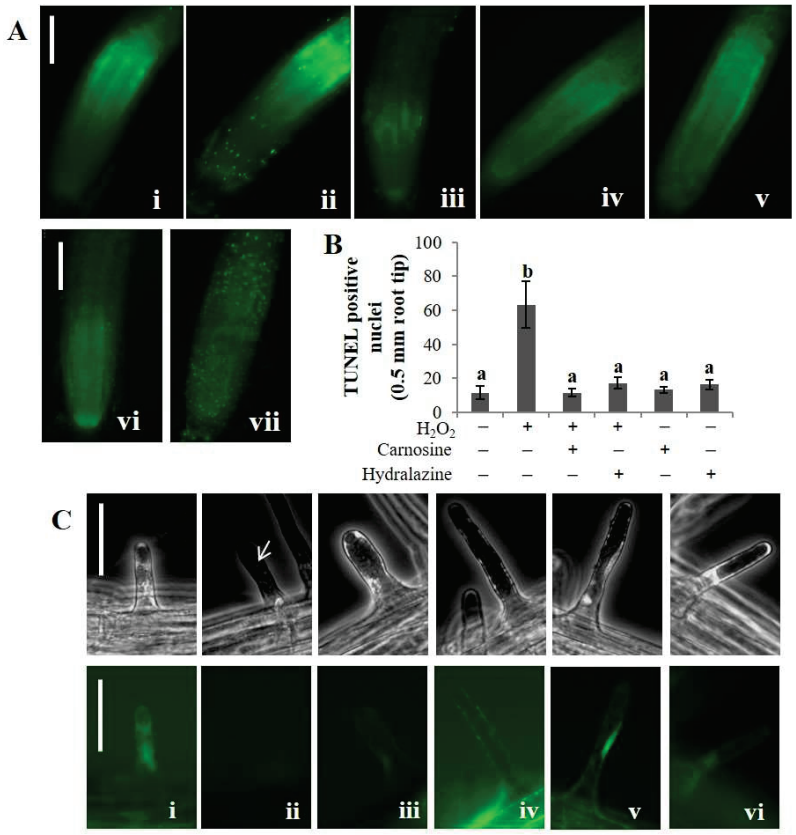

Supplemental Figure S7. H_2O_2-induced PCD in *A. thaliana* roots. Six-d-old plants grown on agar plates were transferred to fresh medium supplemented with 0.2 mM H_2O_2 or a carbonyl scavenger (3 mM carnosine or 0.2 mM hydralazine) or both. After a 20-h incubation, 1 cm of primary root was excised from the tip and used for TUNEL assay and FDA staining as described in the Materials and Methods. (A) Typical fluorescence images for TUNEL assay results: (i) no addition for control, (ii) 0.2 mM H_2O_2, (iii) 0.2 mM H_2O_2 + 3 mM carnosine, (iv) 0.2 mM H_2O_2 + 0.2 mM hydralazine, (v) 3 mM carnosine, (vi) 0.2 mM hydralazine and (vii) DNase I for positive control. Bar, 100 µm. (B) Fraction of the cells with TUNEL-positive nuclei. The total cell number in the root tip of 0.5 mm length excised from the primary root was counted under phase contrast observation, and the TUNEL-positive cells were counted under fluorescence observation. A total of 9 roots were counted in each treatment. Mean of three experiments ± SEM. Differences among treatments were analyzed by Tukey test. $P<0.05$. (C) Typical phase contrast images for cytoplasm retraction (top row) and fluorescence images of the same field (bottom row). From left to right, samples were treated with (i) nothing for blank control, (ii) 0.2 mM H_2O_2, (iii) 0.2 mM H_2O_2 + 3 mM carnosine, (iv) 0.2 mM H_2O_2 + 0.2 mM hydralazine, (v) 3 mM carnosine and (vi) 0.2 mM hydralazine. The white arrow in the panel indicates cytoplasm retraction. Bar, 50 µm.

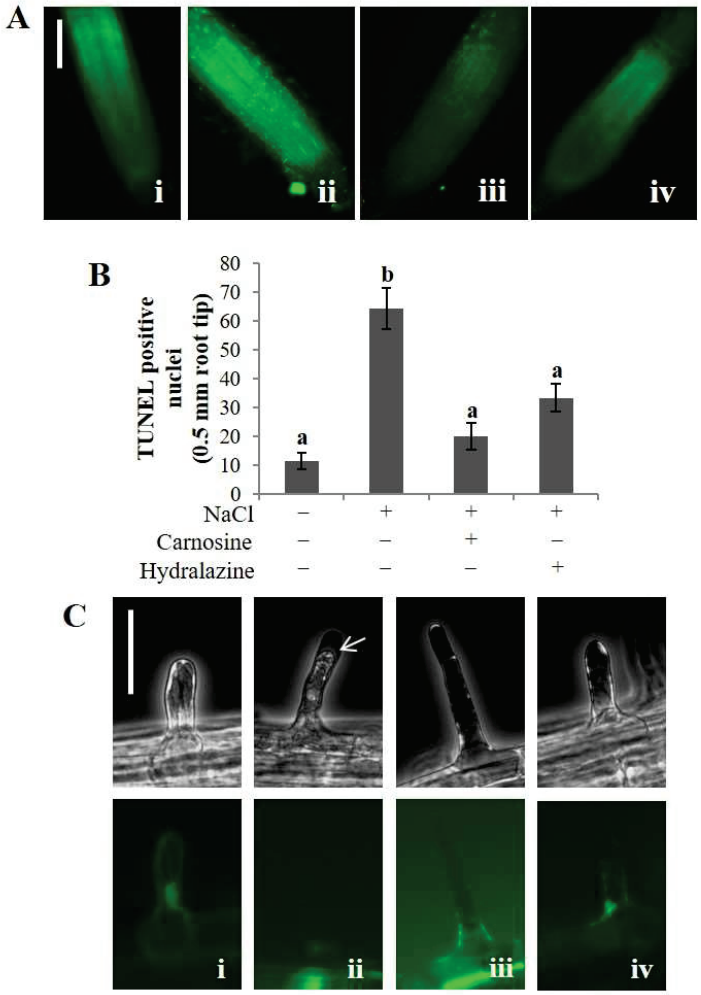

Supplemental Figure S8. NaCl-induced PCD in *A. thaliana* roots. Six-d-old plants grown as in Supplemental Fig. S6 were transferred to fresh MS medium supplemented with either 150 mM NaCl or a carbonyl scavenger (3 mM carnosine or 0.2 mM hydralazine) or both as indicated. After a 20-h incubation, the plants were used for TUNEL assay and FDA staining as described in Materials and Methods. (A) Typical fluorescence images for TUNEL assay results: (i) untreated roots as control, (ii) 150 mM NaCl, (iii) 150 mM NaCl + 3 mM carnosine and (iv) 150 mM NaCl + 0.2 mM hydralazine. Bar, 100 µm. (B) Fraction of the cells with TUNEL-positive nuclei. The total cell number and the TUNEL-positive cells were counted as in supplemental Fig. S6. A total of 9 roots were counted in each treatment. Mean of three experiments ± SEM. Differences among treatments were analyzed by Tukey test. $P<0.05$. (C) Typical phase contrast images for cytoplasm retraction (top row) and fluorescence images of the same field (bottom row). From left to right, samples were treated with (i) untreated roots as control, (ii) 150 mM NaCl, (iii) 150 mM NaCl + 3 mM carnosine and (iv) 150 mM NaCl + 0.2 mM hydralazine. White arrowhead indicates cytoplasm retraction. Bar, 50 µm.

Supplemental Figure S9: Accumulation of carbonyls in *A. thaliana* roots. Six-d-old plants were treated with either 150 mM NaCl or a carbonyl scavenger (3 mM carnosine or 0.2 mM hydralazine) or both as in supplemental Fig S7. After a 20-h incubation, root tip of 1 cm length was excised from the primary root and used for Schiff's staining as described in Materials and Methods. Typical photographs for Schiff's staining: (i) untreated roots as control, (ii) 150 mM NaCl, (iii) 150 mM NaCl + 3 mM carnosine, (iv) 150 mM NaCl + 0.2 mM hydralazine, (v) 3 mM carnosine and (vi) 0.2 mM hydralazine. Bar, 500 µm.

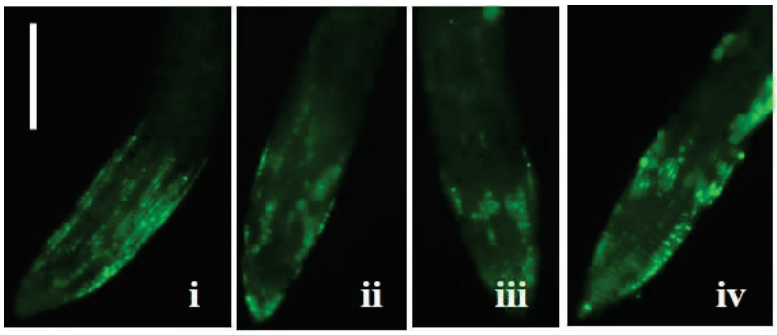

Supplemental Figure S10: Carnosine and hydralazine did not affect the intracellular H_2O_2 level in the root of *A. thaliana.* Six-d-old plants were treated with either 0.2 mM H_2O_2 or a carbonyl scavenger (3 mM carnosine or 0.2 mM hydralazine). After a 20-h incubation, root tips of about 5 mm length were excised from the primary root and used for intracellular H_2O_2 detection with BES-H_2O_2-Ac probe as described in Materials and Methods. Typical photographs are shown: (i) untreated roots as control, (ii) 0.2 mM H_2O_2, (iii) 0.2 mM H_2O_2 + 3 mM carnosine and (iv) 0.2 mM H_2O_2 + 0.2 mM hydralazine. Bar, 250 μm.

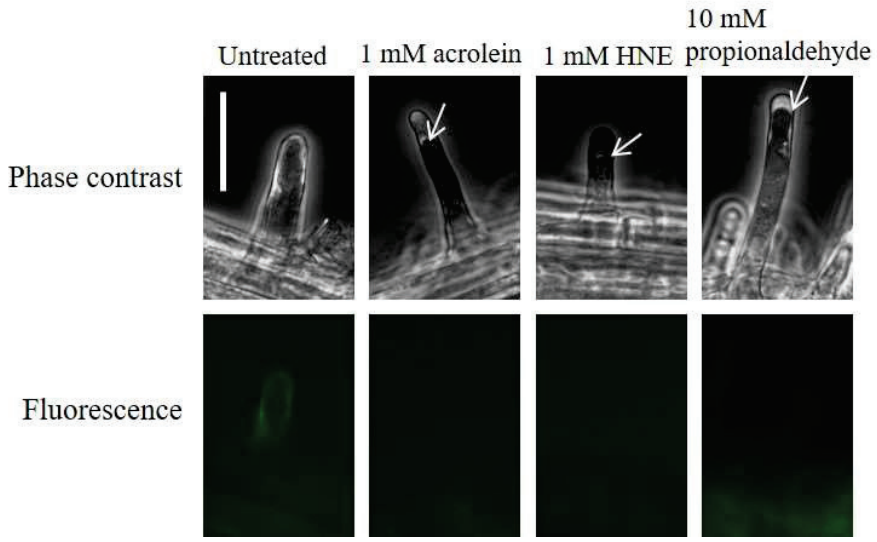

Supplemental Figure S11: Root hair PCD in *A. thaliana* made by carbonyls in the absence of H_2O_2. Six-d-old plants were treated with the indicated carbonyls for 20 h and stained with FDA as described in Materials and Methods. After a 20-h incubation, root tip of 1 cm length was excised from the primary root and used for FDA staining. Typical phase contrast images for cytoplasm retraction (top row) and fluorescence images of the same field (bottom row). Viable root hairs cleave FDA and fluoresce. Phase contrast and fluorescence images of the root hairs were of the same field. The arrowhead indicates cytoplasm retraction. Bar, 50 μm.

Chapter 3

Reactive carbonyl species activate caspase-3-like protease to initiate programmed cell death in plants

3.1 Abstract

Reactive oxygen species (ROS)-triggered programmed cell death (PCD) is a typical plant response to biotic and abiotic stressors. We have recently shown that lipid peroxide-derived reactive carbonyl species (RCS), downstream products of ROS, mediate oxidative signal to initiate PCD. Here we investigated the mechanism by which RCS initiate PCD. Tobacco Bright Yellow-2 cultured cells were treated with acrolein, one of the most potent RCS. Acrolein at 0.2 mM caused PCD in 5 h (i.e. lethal), but at 0.1 mM it did not (sub-lethal). Specifically, these two doses caused critically different effects on the cells. Both lethal and sub-lethal doses of acrolein exhausted the cellular glutathione pool in 30 min, while lethal dose only caused a significant ascorbate decrease and ROS increase in 1-2 h. Prior to such redox changes, we found, acrolein caused significant increases in the activities of caspase-1-like protease (C1LP) and caspase-3-like protease (C3LP), the proteases to trigger PCD. The lethal dose of acrolein increased the C3LP activity twofold greater than did the sub-lethal dose. In contrast, C1LP activity increment by the two doses were not different. Acrolein and 4-hydroxy-(*E*)-2-nonenal, another RCS, activated both proteases in cell-free extract from untreated cells. H_2O_2 at 1 mM added to the cells increased C1LP and C3LP activities and caused PCD, and the RCS scavenger carnosine suppressed their activation and PCD. However, H_2O_2 did not activate the proteases in cell-free extract. Thus the activation of caspase-like proteases, particularly C3LP, by RCS is an initial biochemical event in oxidative signal-simulated PCD in plants.

3.2 Introduction

The production of reactive oxygen species (ROS), such as superoxide radical (O_2^{-}),

hydrogen peroxide (H_2O_2), and singlet oxygen ($^1O_2$) is intrinsically associated with photosynthesis, photorespiration and respiration (Foyer and Noctor 2003, Asada 2006). ROS have various biological roles ranging from defense signal to destructive agents, depending on their levels and the way of their production (Mittler et al. 2011). Plant cells contain abundant antioxidant molecules such as the reduced form of glutathione (GSH) and ascorbic acid (Asc), and an array of ROS-scavenging enzymes such as superoxide dismutase and ascorbate peroxidase (Asada 1999). As a result, the intracellular ROS levels are determined by the balance between their production and scavenging. Under mild stress conditions, the ROS level increases gradually, and O_2^- and H_2O_2 at relatively low concentrations activate a battery of defense genes (Miller et al. 2010). When a plant is exposed to severe and prolonged abiotic stress, its antioxidant capacity is decreased and the ROS levels are further increased, leading to cell death (Mano 2002). In response to attack by pathogens including bacteria, fungi and viruses, the infected cells produce transiently as 'oxidative burst' via the activation of the respiratory burst oxidase homologs (Levine et al. 1994, Torres and Dangl 2005). This type of ROS formation leads to death of the original and neighboring cells and induces defense responses in the surrounding uninfected cells (Torres et al. 2005). These various effects of ROS are collectively designated as oxidative signaling (Mittler et al. 2011).

Programmed cell death (PCD) is one of the typical consequences of oxidative signaling (Van Breusegem and Dat 2006, Petrov et al. 2015). For example, in tobacco (*Nicotiana tabacum*) Bright Yellow-2 (BY-2) cells, an increase in the O_2^- level is necessary for execution of PCD on salt and sorbitol stress (Monetti et al. 2014). Short-term drought on developing anthers in rice (*Oriza sativa*) increases the level of H_2O_2 and decreases the level of transcripts of antioxidant enzymes, and thereby leads to PCD (Nguyen et al. 2009). High temperature treatment of tobacco cells increases the H_2O_2 level before PCD occurs (Locato et al. 2008). Hypersensitive response (HR)-like cell death, a typical PCD in tobacco leaves, is also caused by H_2O_2 (Yoda et al. 2003). There is keen interest in the biochemical mechanism by which

ROS initiate PCD (Apel and Hirt 2004, de Pinto et al. 2012, Petrov et al. 2015).

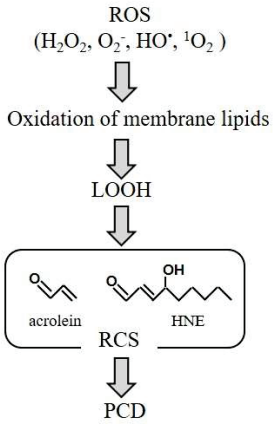

Fig. 1 Generation of RCS under oxidative stress. From various species of LOOH, dozens of oxylipin carbonyls (LOOH-derived aldehydes and ketones) are formed enzymatically or by redox catalysts such as transition metal ions or free radicals. Among them, those carbonyl species comprising the α,β-unsaturated bond, such as acrolein and HNE, are highly electrophilic and designated as reactive carbonyl species (RCS).

To investigate the mechanism of oxidative signal-induced PCD, we previously tested the hypothesis that oxylipin carbonyls are signal mediators. Oxylipin carbonyls collectively designate the aldehydes and ketones produced from lipid peroxides (LOOH) (Fig. 1). They are produced in abiotic stressed plants and mediate tissue damage (Yin et al. 2010, Mano et al. 2010, Yamauchi et al. 2015) via protein modification (Winger et al. 2007, Mano et al. 2014), and therefore they are strong candidates of oxidative signal mediators (Mano 2012, Farmer and Mueller 2013). We recently examined the roles of oxylipin carbonyls in PCD in tobacco and *A. thaliana*, and obtained following results (Biswas and Mano 2015). (i) When tobacco BY-2 cells were treated with H_2O_2 at the level that cause PCD, several species of oxylipin carbonyls were increased prior to the progression of the cell death. (ii) These species of oxylipin carbonyls, when exogenously added, induced PCD in BY-2 cells and roots of tobacco and *A. thaliana*. (iii) Carbonyl-scavenging compounds suppressed the accumulation of oxylipin carbonyls and PCD in H_2O_2-treated BY-2 cells and *A. thaliana* roots, without

affecting the ROS increase and LOOH accumulation. We further demonstrated that (iv) a transgenic tobacco line that overproduces 2-alkenal reductase, an *A. thaliana* enzyme to detoxify *α,β*-unsaturated carbonyls (Mano et al. 2012), showed significantly smaller increase in the levels of oxylipin carbonyls and they suffered less cell injury in root epidermis after H_2O_2 and salt treatments than wild type (Biswas and Mano 2015). These results indicate that oxylipin carbonyls, endogenously produced due to the H_2O_2 stimulus, mediated the oxidative signal to induce PCD in plant cells.

The purpose of this study is to elucidate the mechanism by which oxylipin carbonyls trigger PCD. Here we employed an experimental system of PCD induced in BY-2 cells by reactive carbonyl species (RCS). RCS designates the oxylipin carbonyls comprising the *α,β*-unsaturated bond (Mano et al. 2012), which are more potent electrophiles than simple aldehydes or ketones (Fig. 1). In H_2O_2-stimulated BY-2 cells, two RCS acrolein and HNE were increased in early stages, and they showed stronger effects to cause PCD than any other oxylipin carbonyls found in H_2O_2-stimulated cells (Biswas and Mano 2015). In the present study, we found that acrolein caused depletion of the GSH pool in BY-2 cells, then gradually lowered the ascorbate level and enhanced the ROS level. Importantly, caspase-1-like protease (C1LP) and caspase-3-like protease (C3LP), both of which are involved in triggering PCD, were activated rapidly after acrolein addition. These results reveal the biochemical mechanisms of the RCS-mediated initiation of PCD in plants.

3.3 Results

3.3.1 Effects of acrolein on cell viability of cultured tobacco BY-2 cells

To determine the concentration limit of acrolein to trigger PCD, we treated cells with acrolein at various concentrations. Cell viability was determined by fluorescein diacetate (FDA), which is membrane permeable and fluoresces only in living cells due to the cleavage by intracellular esterases. When acrolein at 0.1 mM was added to BY-2 cells, the viability was

reduced by 10% in 5 h, not significantly different from that obtained for untreated cells. In 0.2 mM acrolein, BY-2 cells started to die in 30 min and about 75% cells were dead in 5 h (Fig. 2A). Cellular protein content is another maker of cell viability. Acrolein at 0.1 mM did not cause a decrease in the protein level even after 5 h incubation, while the agent at 0.2 mM decreased it in 30 min, and after 5 h-incubation protein was lost by more than 60% (Fig. 2B). Analyses of these two parameters indicate that tobacco BY-2 cells survived in 0.1 mM acrolein, but they suffer irreversible cell death in 0.2 mM. This acrolein-induced cell death is typical PCD characterized by DNA-fragmentation, cytoplasm retraction and the terminal deoxynuleotidyl transferase dUTP nick end labeling-positive nuclei, as we have previously shown (Biswas and Mano 2015). Considering that acrolein at 0.2 mM was a lethal dose and the agent at 0.1 mM was sub-lethal, we examined the difference in the effects of these two critical doses on BY-2 cells.

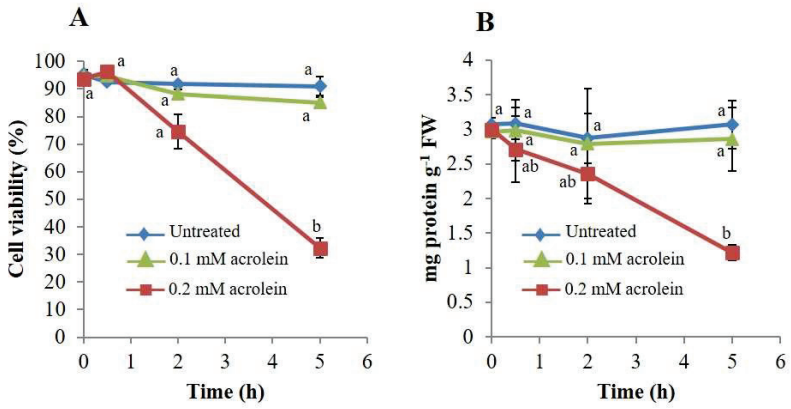

Fig. 2 Effects of acrolein on the viability and protein content of tobacco BY-2 cells. Fifty mg of cells from 7-d culture were sub-cultured in 50 mL fresh culture media, and after 4 days the culture medium was supplemented with acrolein at 0.1 mM and 0.2 mM. Cells were harvested at the indicated time point then living cell (A) and protein content (B) were determined as described in Materials and Methods. Each point represents the mean of three independent experiments and the error bars of the SEM. Differences among treatments were analyzed by Tukey test. $P<0.05$.

3.3.2 Acrolein depletes intracellular glutathione and ascorbate

Thiol compounds such as the reduced form of glutathione (GSH) provide the first defence

against electrophiles including RCS (Esterbauer et al. 1975, Mano et al. 2009). Because the intercellular concentration of GSH and the glutathione reduction ratio (GSH/(GSH + oxidized glutathione)) determine the redox homeostasis of the cell (Foyer and Noctor 2011), the consumption of GSH would affect the cells considerably. In the BY-2 cells treated with lethal level of acrolein, i.e., 0.2 mM, GSH was decreased by 95% in 30 min (Fig. 3A). The lowered level did not recover afterwards. The GSH reduction ratio was also dropped significantly in 30 min, and the lowered level was retained (Fig. 3B). Interestingly, even sub-lethal level of acrolein, i.e., 0.1 mM, caused very similar effects on the GSH content and the reduction level. In 0.1 mM acrolein, 95% of the cellular GSH pool was lost and the reduction level was lowered to a half in 30 min. These lowered levels did not recover even at 5 h, the time at which more than 80% of the cells were alive (Fig. 2). These results indicate that the rapid drop of the intracellular GSH pool caused by acrolein, although it is drastic and persistent, does not directly initiate PCD.

Acrolein at 0.05 mM decreased the GSH content to 15% of the untreated cells in 30 min, and after that the pool was restored to 80% in 5 h (Fig. 3A). The GSH reduction ratio was dropped to 50%, and then it recovered to 70% (Fig. 3B). A large recovery of the GSH pool is an reflection of active *de novo* synthesis of GSH in acrolein-treated cells.

We also examined changes in the Asc content (Fig. 3C) and the reduction ratio (Asc / Asc + dehydroascorbate (DHA)) (Fig. 3D). In acrolein at 0.1 mM or higher, GSH is extensively consumed (Fig. 3A), and hence the regeneration of Asc from DHA via the DHA reductase reaction (Asada 1999) would be eliminated. Because Asc do not directly scavenge acrolein (Mano et al. 2009), the Asc content under such conditions therefore reflects the balance between the Asc oxidation by ROS and the *de novo* synthesis of Asc. Acrolein at the lethal level (0.2 mM) caused a decrease in the Asc content by 30% in 30 min and significantly lowered it in 2 h and 5 h (Fig. 3C). Ascorbate reduction ratio was also decreased in 2 h (Fig.

3D). The sub-lethal level of acrolein (0.1 mM) tended to decreased the Asc level, but the decrease was apparently smaller than that observed for the 0.2 mM acrolein-treatment (Fig. 3C). Ascorbate reduction ratio was also decreased by 5% in 0.1 mM acrolein in 30 min, and it was not significantly different from that in 0.2 mM acrolein-treated cells (Fig. 3D). These results suggest that there is a difference between the lethal and sub-lethal conditions in either the Asc oxidation rate or Asc synthesis rate, or both.

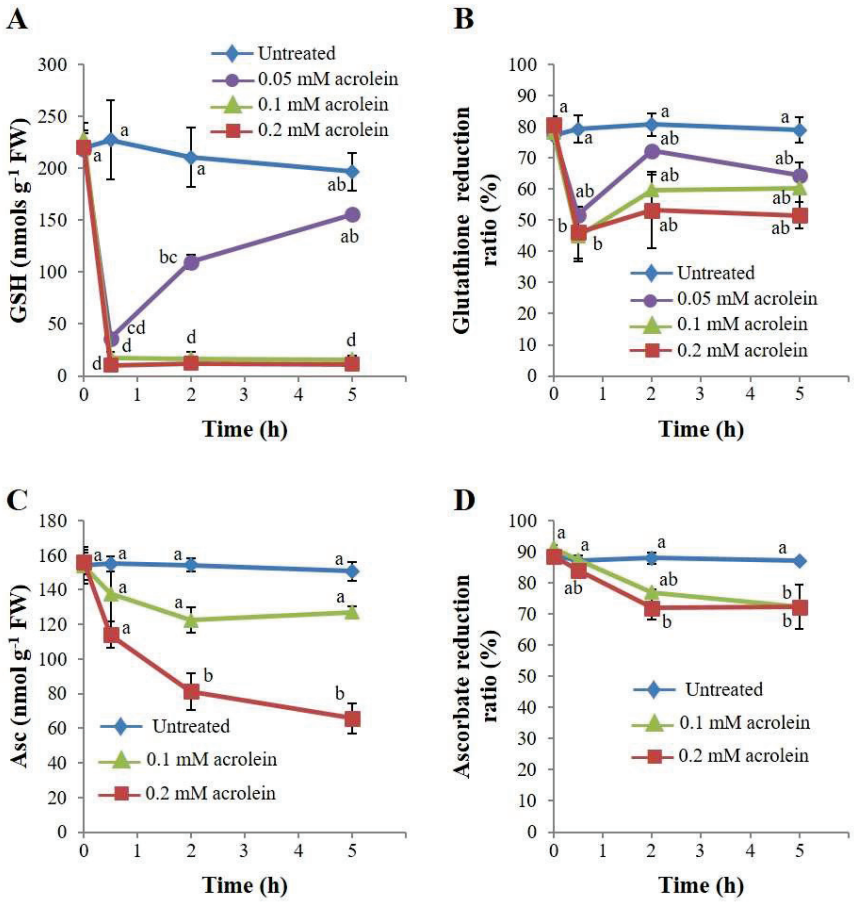

Fig. 3 Effects of acrolein on the contents and the reduction ratio of GSH and Asc in BY-2 cells. Four-d cultured cells were treated with various concentration of acrolein and then used as in Fig. 1. (A) contents of reduced glutathione (GSH), (B) GSH reduction ratio (%), (C) reduced ascorbate (Asc) and (D) Asc reduction ratio. Each point represents the mean of three independent experiments and the error bars of the SEM. Different letters represent significant different data ($P<0.05$ on Tukey test).

3.3.3 Acrolein treatment increased ROS level in BY-2 cells

The loss of GSH and Asc pools in acrolein-treated cells should cause oxidative load in cells. We then investigated the effects of acrolein on the ROS level in BY-2 cells with the probe 2′,7′-dihydrodichlorofluoresein-diacetate (H_2DCF-DA). The intracellular oxidation of H_2DCF to the fluorescent dichlorofluorescein (DCF) is a marker of the generation of ROS such as superoxide radical, H_2O_2 and hydroxyl radical. When BY-2 cells were exposed to acrolein at 0.1 mM for 60 min, the level of DCF fluorescence was 1.7-fold higher than the untreated cells (Fig. 4). Acrolein at 0.2 mM in 30 min resulted in 1.5-fold higher and after 60 min resulted in 2.3-fold higher DCF fluorescence, a significant difference from the untreated control (Fig. 4B). Thus the increase in the ROS was obviously slower than the GSH consumption, and appears to reflect the loss of Asc pool. Thus acrolein promotes oxidative stress in an indirect, feed-forward manner.

A

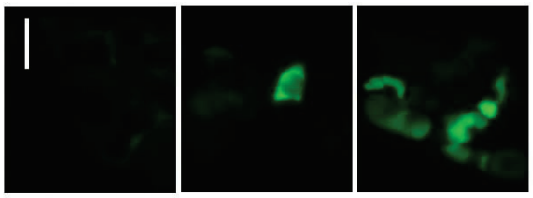

B

	Time of incubation (min)		
Acrolein	0	30	60
0.1 mM	101 ± 26[a]	–	182 ± 22[ab]
0.2 mM	96 ± 17[a]	153 ± 3[ab]	234 ± 16[b]

Fig. 4 Acrolein increases the ROS level in BY-2 cells. (A) Four-d-cultured cells were incubated with 0.1 mM acrolein for 30 min and 0.2 mM acrolein for 30 min and 60 min. DCF fluorescence was recorded under a fluorescence microscope as in Materials and Methods. Typical photographs are shown: untreated cells as control (left), and treated with acrolein at 0.1 mM (middle) and 0.2 mM (right). Bar, 50 μm. (B) The DCF fluorescence intensity of cells (%). The fluorescence intensity was integrated per cell with ImageJ software. A total of 200 cells were counted in each treatment. Mean ± SEM of three independent experiments. Differences among treatments were analyzed by Tukey test. $P<0.05$.

3.3.4 Activation of caspase-like proteases by acrolein in BY-2 cells

In mammalian cells, the most characterized form of PCD is apoptosis that is executed by highly conserved cysteine-containing aspartate-specific proteases (caspases) (Shi 2002). Caspases are numbered according to their specificity to artificial peptide substrates. Plants do not have structural homologs of caspases, but have the protease activities with similar substrate specificity to those of animal caspases. In pathogen-induced PCD in plants, the activity of caspase-1-like protease (C1LP) is increased and the caspase-1 inhibitor activity of caspase-1-like protease (C1LP) is increased and the caspase-1 inhibitor suppresses the development of PCD in tobacco (del Pozo and Lam 1998, Hatsugai et al. 2004). The C1LP activity is at least partially attributed to vacuolar processing enzymes (VPE), an orthologs of asparaginyl endopeptidase (legumain). VPEs are localized in the vacuole and responsible for processing vacuolar proteins (Hatsugai et al. 2004). Thus the contribution of C1LP to plant PCD compares with the animal caspase-1 as a cell death executor (Hatsugai et al. 2015). Caspase-3-like protease (C3LP) activity is involved in HR-induced or abiotic stress-regulated PCD (Fernández et al. 2012, Ye et al. 2013). It can be attributed to the 20S proteasome subunit PBA1 (Han et al. 2012, Hatsugai et al. 2009). Because ROS stimulate plant cells to increase the activities of these proteases (Clarke et al. 2000, Locato et al. 2008), we examined whether RCS, as oxidative signal, have similar effects or not.

The C1LP and C3LP reactions were monitored using the fluorogenic substrates *N*-acetyl-Tyr-Val-Ala-Asp-α-(4-methyl-coumaryl-7-amide) (Ac-YVAD-AMC) and *N*-acetyl-Asp-Glu-Val-Asp-AMC (Ac-DEVD-AMC), respectively. The activities were determined by subtraction of the fluorescence intensity after a 1 h-enzymatic reaction in the presence of the inhibitor from that in its absence. In the untreated cells, there were constitutive activities of C1LP and C3LP (Fig. 5). These activity levels did not change during the experimental period in untreated cells and hence are irrelevant to PCD. In the cells treated with the lethal level of acrolein (0.2 mM), a significant increase in the C1LP activity was

detected in 30 min; it reached a twofold of the constitutive level, and the raised activity was kept up to 60 min (Fig. 5A). This activation of C1LP is not sufficient to cause PCD because a similar extent of activation was observed even in a sublethal concentration (0.1 mM) acrolein.

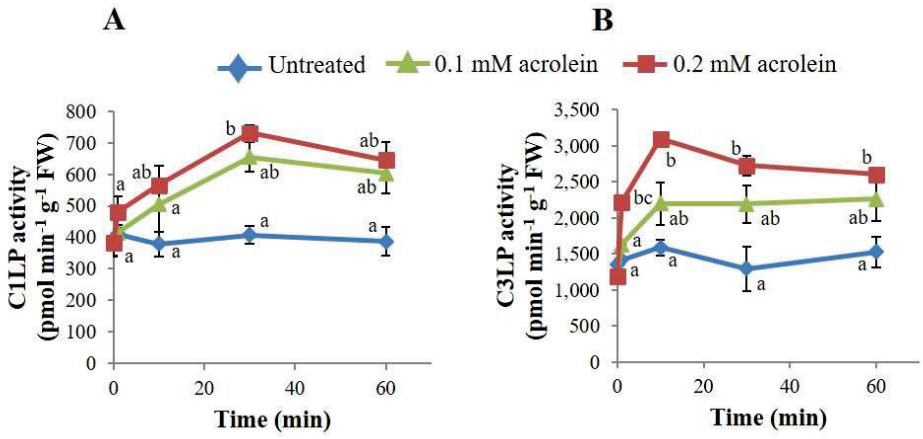

Fig. 5 Activation of C1LP (A) and C3LP (B) in BY-2 cells after exposure to acrolein. Four-d cultured cells were treated with 0.1 mM and 0.2 mM acrolein. Protease inhibitors were added to cell extracts to a final concentration of 0.1 mM and caspase assay was performed using fluorogenic substrates Ac-YVAD-AMC for C1LP (A) and Ac-DEVD-AMC for C3LP (B) as in Materials and Methods. The data are the mean ± SEM. Different letters represent significant different data ($P<0.05$ on Tukey test).

The C3LP activity was also increased in the lethal acrolein concentration (Fig. 5B). In 10 min, its activity reached 3,000 pmol min^{-1} (g FW)$^{-1}$. The increase from the constitutive level (1,200 pmol min^{-1} (g FW)$^{-1}$) was 2,800 pmol min^{-1} (g FW)$^{-1}$. Even in 1 min, a significant increase was detected. In the sub-lethal acrolein concentration C3LP was also activated, but the increase from the constitutive level was less than 1,200 pmol min^{-1} (g FW)$^{-1}$. Thus the increase in the C3LP activity under the lethal condition was more than twofold than that under the sub-lethal condition. It appears that the activation of C3LP to such a level is critical to the initiation of PCD.

3.3.5 H_2O_2-induced activation of C1LP and C3LP in BY-2 cells is suppressed by the RCS scavenger carnosine

The C1LP and C3LP activities would be increased also in H_2O_2-stressed cells because the PCD caused by H_2O_2 is ascribed to the action of RCS (Biswas and Mano 2015). Exposure of the cells to 1 mM H_2O_2, the concentration high enough to induce PCD in BY-2 cells, resulted in significant increases of C3LP activity in 1 min, and then they reached plateau (Fig. 6). The reached activity levels were 2.7-fold higher for C1LP and 1.9-fold higher for C3LP, than the corresponding untreated controls. Thus C1LP and C3LP activities were increased in very early stages of the H_2O_2-induced PCD. To verify the involvement of RCS, we tested the effects of the RCS-scavenging dipeptide carnosine. Carnosine suppresses the increase in RCS levels in H_2O_2-treated BY-2 cells, without affecting the intracellular ROS level (Biswas and Mano 2015). The concentration used here (1 mM) is high enough to eliminate the H_2O_2-induced PCD (data not shown). In the presence of carnosine, as expected, the increase in the C1LP activity was significantly suppressed (Fig. 6A). The increase in the C3LP activity was also suppressed, but only partially (Fig. 6B). Thus the increase in the C1LP activity in H_2O_2-stimulated BY-2 cells is attributed mostly to the endogenously generated RCS, and so is that of the C3LP activity, at least partially.

Thus both acrolein and H_2O_2 caused increases in the C1LP and C3LP activities in BY-2 cells. The C3LP activity increase from the constitutive activity was twofold higher under lethal conditions (0.2 mM acrolein or 1 mM H_2O_2) than its increase under sub-lethal condition (0.1 mM acrolein or 1 mM H_2O_2 + 1 mM carnosine). Significant activity increases were observed in 10 min in both treatments. It appears that the increase in the C3LP activity over such a threshold in a very early stage of stress treatment is required for the subsequent progress of PCD.

3.3.6 RCS directly activate C1LP and C3LP

To investigate the mechanism by which acrolein and H_2O_2 increase the C1LP and C3LP activities, proteins were extracted from the cells and the effects of these agents on the protease

activities *in vitro* were examined. Acrolein at 0.05 mM was added to the cell-free extract prepared from non-stressed BY-2 cells. After removing acrolein through gel filtration, the C1LP and C3LP activities were determined (Fig. 7). It was found that acrolein activated both proteases up to twofold as compared with the basal levels. Not only acrolein, but also HNE, another RCS, did activate both C1LP and C3LP to the same extents (Supplemental Fig. S1). These results indicate that RCS acted directly on the C1LP and C3LP proteins, and activated them.

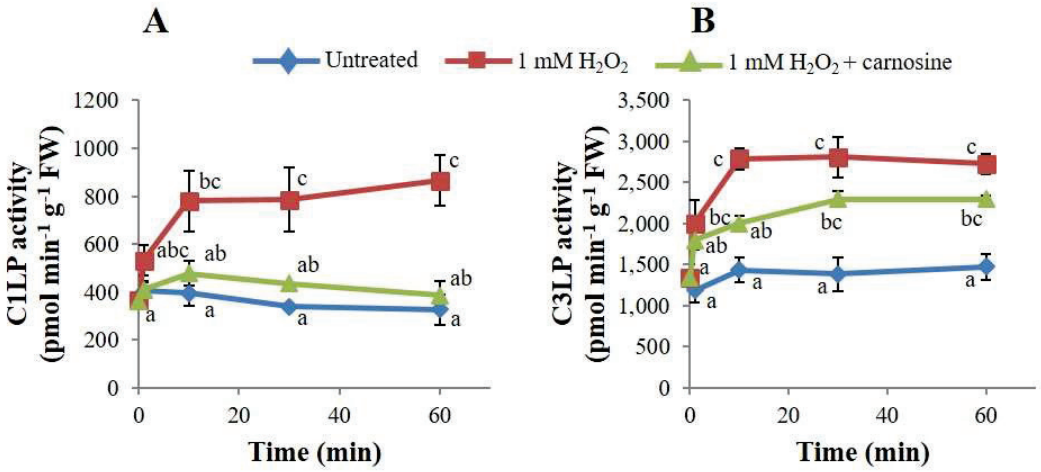

Fig. 6 H_2O_2 increased the C1LP (A) and C3LP (B) activities in BY-2 cells, and carnosine suppressed their increases. Four-day cultured cells were treated with either 1 mM H_2O_2 or 1 mM H_2O_2 plus 1 mM carnosine at the indicated time. The data are the mean of three independent experiments ± SEM. Different letters represent significant different data ($P<0.05$ on Tukey test).

As shown in Fig. 5, the C3LP activity in BY-2 cells became double by 0.2 mM acrolein. In vitro, in contrast, C3LP was not increased significantly in 0.2 mM acrolein (Fig. 8). Acrolein at 0.1 mM or higher concentration also inactivated C1LP (data not shown). These different concentration dependencies of the activation of C1LP and C3LP between the *in vivo* and *in vitro* conditions were most probably due to the difference in the effective acrolein concentrations between two experimental systems (discussed below).

On the other hand, H_2O_2 at 0.05 mM or higher concentration in cell-free extract did not activate C3LP (Fig. 8) and C1LP (data not shown). The activation of C1LP and C3LP in the H_2O_2-treated BY-2 cells (Fig. 6) is therefore attributed solely to the action of RCS that are generated downstream of ROS, and the possibility that H_2O_2 directly activated these proteases is excluded.

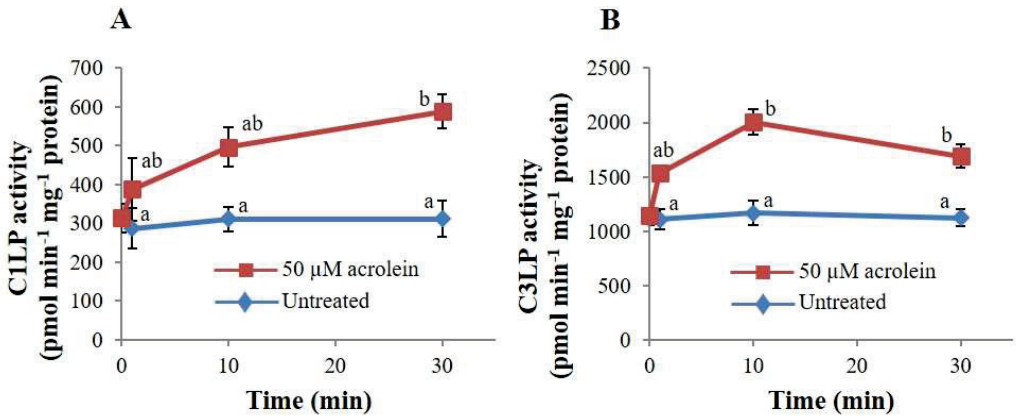

Fig. 7 Activation of C1LP (A) and C3LP (B) by acrolein in cell-free extract. Protein was extracted from the 4-day cultured cells and desalted against 50 mM sodium acetate, pH 5.5 by gel filtration as in Materials and Methods (cell-free extract). Acrolein was added to the cell-free extract (1.06 mg protein mL^{-1}), and C1LP (A) and C3LP (B) activity were measured as in Materials and Methods. Data are the mean ± SEM. Different letters represent significant different data ($P<0.05$ on Tukey test).

3.3.7 Acrolein enhances the expression of VPE genes in BY-2 cells

VPE genes are up-regulated in the vacuolar cell death process in rice after exposure to H_2O_2 (Deng et al. 2011) and Al-stressed BY-2 cells (Kariya et al. 2013). We then investigated whether acrolein induces the expression of VPE genes. Acrolein at 0.2 mM was added to BY-2 cells, and the expression of the four tobacco VPE genes (*VPE1a, VPE1b, VPE2* and *VPE3*) was assessed. We found that all the four VPE genes were up-regulated slightly, but insignificantly after 30 min exposure with acrolein (Fig. 9A). After 60 min exposure the expression of *VPE1a* and *VPE1b* were up-regulated by 3- and 4-fold than the untreated cells, respectively (Fig. 9B). The expression of *VPE2* and *VPE3* were also up-regulated, but the

enhancement was insignificant (Fig. 9B). These results indicate that acrolein induces the expression of *VPE1a* and *VPE1b* genes. Their up-regulation was apparently slower than the rise of C1LP activity, which occurred within 30 min (Fig. 5). The rapid activation of C1LP in acrolein-treated cells is therefore primarily accounted for by the direct biochemical activatization of the C1LP protein by acrolein (Fig. 7).

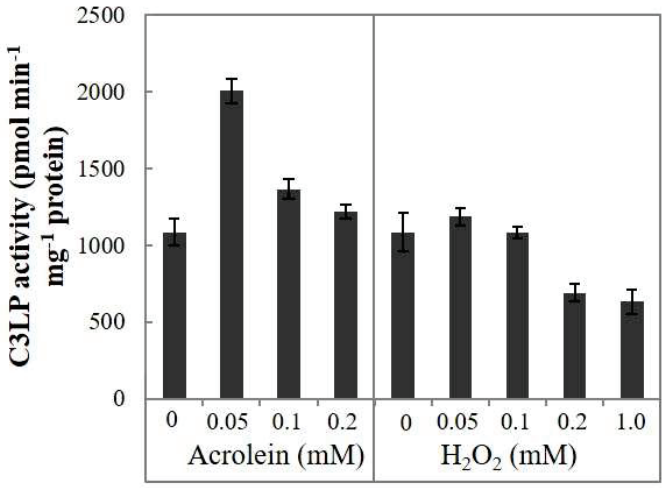

Fig. 8 Effects of various concentration of acrolein and H_2O_2 on the activation of C3LP in cell-free extract. Protein was extracted from the 4-day cultured cells. H_2O_2 and acrolein were added at the indicated concentration in 1 mL protein extract (1.06 mg mL^{-1}) and desalted as in Materials and Methods. The data are the mean ± SEM of three independent experiments.

3.4 Discussion

3.4.1 Activation of C3LP is the earliest event in acrolein-induced PCD

On our recent finding that RCS mediate the oxidative signal to induce PCD in plants (Biswas and Mano 2015), in this study, we aimed at investigating the mechanism by which RCS initiate PCD in tobacco BY-2 cells. Acrolein, one of the most potent RCS, had multiple effects on the cells, i.e., decreasing the glutathione and ascorbate levels, increasing the activity of two caspase-like proteases C1LP and C3LP and inducing the expression of *VPE1a* and *VPE1b* genes. We consider that the C3LP activity increase was the most critical event for the initiation of PCD, for the following reason. To BY-2 cells, 0.2 mM acrolein was lethal and

it caused death to 95% population of the cells in 5 h. The treatment with 0.1 mM acrolein was sub-lethal; 80% population was alive in 5 h, a viability comparable to that of untreated control cells. In the lethal concentration of acrolein, following biochemical events were observed in the cells. (i) GSH was exhausted in 30 min, and the lowered level did not recover. (ii) Asc level was decreased to a half in 2 h. (iii) C1LP activity was increased to a double of its constitutive level in 30 min. (iv) C3LP activity was increased to a double of its constitutive level in 1 min, and reached to a 2.7-fold in 10 min. The sub-lethal concentration of acrolein also caused the events (i) and (iii) to the same extents. Specifically, the GSH consumption and the increase in the C1LP activity are not sufficient conditions for the initiation of PCD. On the other hand, the Asc decrease was obviously smaller, and the C3LP activity increase was a half maximal in the sub-lethal acrolein concentration, as compared with those in the cells under PCD. Thus the increase in the C3LP activity was more closely associated, than that in the C1LP activity, with the initiation of PCD. When the lethal level of acrolein was added, the C3LP activity was increased much faster than the Asc pool was decreased significantly. Taking these results together, we conclude that the early increase in the C3LP activity determined the cell fate.

3.4.2 RCS-mediated activation of caspase-like proteases is a mechanism of ROS-induced PCD

We also found that a lethal level of H_2O_2 increased the C1LP and C3LP activities in the cells. Carnosine, an RCS scavenger, suppressed these increases and also PCD. Because carnosine does not scavenge H_2O_2 and other ROS in the cells (Biswas and Mano 2015), it was unlikely H_2O_2 had a direct effect to activate these proteases. This is supported by the result that H_2O_2 did not increase the activity of C1LP and C3LP in cell-free extract (Fig. 8) while acrolein and HNE did it (Fig. 7, Supplementary Fig. S1). These results indicate that RCS mediated the oxidative signal to cause PCD by activating C1LP and C3LP.

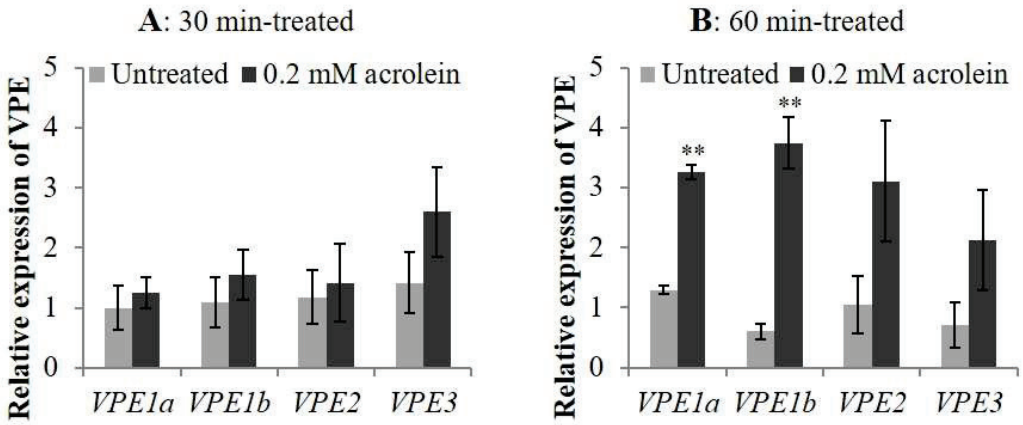

Fig. 9 Acrolein enhanced the expression of VPE genes in BY-2 cells. Four-d cultured cells were treated with 0.2 mM acrolein for 30 min (A) and 60 min (B), then total RNA was isolated. Expression level of *VPE1a*, *VPE1b*, *VPE2* and *VPE3* were determined by real-time quantitative RT-PCR as described in Materials and Methods. Expression of ACT9 gene was used as internal standard. The data are the mean ± SEM of three independent experiments. The asterisks indicate significance difference between untreated and acrolein-treated samples by Student's *t*-test, $^{**}P<0.01$.

For BY-2 cells, the acrolein concentration to fully increase the C1LP and C3LP activities was 0.2 mM, but in cell-free extract, the optimal concentration to activate these activities was 0.05 mM. This difference in the concentration dependencies between *in vivo* and *in vitro* conditions was probably due to the difference in the actual concentration of acrolein, as follows. Because acrolein is scavenged by GSH, its concentration in cells should be much lower than that outside in the medium. A large recovery of the GSH pool in the cells treated with 0.05 mM acrolein (Fig. 2A) indicates a continuous GSH supplementation via *de novo* synthesis; the lowered GSH level was restored after all acrolein was scavenged. Thus the supply of GSH by *de novo* synthesis affects the intracellular acrolein concentration. In 0.1 mM acrolein treatment, continuous *de novo* synthesis of GSH probably contributed to suppressing the intracellular acrolein concentration to a level just lower than that required for triggering PCD. In 0.2 mM acrolein, the GSH biosynthesis flux probably overwhelmed by the consumption flux. As a result, intracellular acrolein concentration would reach the level to activate C1LP and C3LP.

Increase in the C3LP activity is associated with the PCD in heat shocked BY-2 cells (Vacca et al. 2007) and the cadmium-induced PCD in *A. thaliana* (Ye et al. 2013). Chilling and starvation stress in the microspore of barley accumulated H_2O_2 and increased the C3LP activity, leading to PCD (Rodriguez-Serrano et al. 2011). Bacteria-induced PCD in tobacco leaves was abolished by a C3LP inhibitor (del Pozo and Lam 1998). C3LP activity was increased in bacterial pathogen induced-HR in *A. thaliana* (Hatsugai et al. 2009). ROS are involved in many case of such plant PCD caused by biotic and abiotic stressors (Petrov et al. 2015). In the megagametophyte death during post-germinative seedling growth of white spruce, ROS dependence (He and Kermode 2010), and requirement for a rise in the C3LP activity (He and Kermode 2003) are also reported. Because RCS are formed inevitably downstream of ROS (Mano 2012), it is highly likely that they cause the increase in the C3LP activity also in such developmental types of ROS-induced PCD.

The critical involvement of the C1LP activity in many types of PCD has been demonstrated on the inhibition of PCD by a C1LP inhibitor or by the deficiency of the *VPE* gene (Hatsugai et al. 2015). In the current study, we judged that the increase in the C1LP activity was not sufficient to cause PCD because it was also observed under a sub-lethal condition (Fig. 5A). Under lethal condition *VPE1a* and *VPE1b* genes were up-regulated in 60 min where in 30 min up-regulation was insignificant (Fig. 9). Thus increased activity of C1LP and up-regulation VPE genes, however, might be a necessary condition for PCD, in combination with that of C3LP.

3.4.3 C3LP and C1LP are activated *in vitro* by RCS

In apoptosis of mammalian cells, caspases are activated from latent forms and exert their protease activities. For example, various stimuli such as oxidative agents and cytochrome *c* released from mitochondria activate caspase-9, which in turn activates caspase-3 via the cleavage of its inactive pre-protein procaspase-3. The active caspase-3 then acts as an effector

caspase to degrade various target proteins and facilitate the death program (Shi 2004). Because plant caspase-like proteases are structurally unrelated with mammalian caspases, they would be activated in a different way from that of mammalian caspases. In this study, we found that RCS rapidly increased the C3LP and C1LP activities in cell-free extract, indicative of the activation without gene expression/*de novo* protein synthesis. Such activation of caspase-like proteases by the action of RCS will provide a key to the mechanism of oxidative signal-induced PCD.

3.4.4 Signaling role of carbonyls

Recently, evidence is accumulating that various carbonyl compounds act as signals in plants. For example, acrolein can inhibit stomata opening at physiological concentrations (Islam et al. 2015). Because ROS are generated in guard cells by the abscisic acid stimulus (Pei et al. 2000), it is likely that acrolein and other RCS are produced and inhibit stomata opening, thereby acting as a signal for stomata closure. In heat shock-response also RCS are involved (Yamauchi et al. 2015). Interestingly, the species to mediate the heat shock response are limited to RCS of carbon chain length 4-9. Acrolein, the C3 RCS, is unable to act as the heat shock signal. This implies that, in distinct carbonyl signaling responses, putative carbonyl receptors have specificities to distinguish various carbonyl species.

Besides RCS, which are derived from lipid peroxides, dicarbonyl species such as methylglyoxal and glyoxal are formed as inevitable by-products in sugar metabolism including the Calvin cycle (Takagi et al. 2014). Methylglyoxal, when produced in chloroplasts, can mediate the photoreduction of O_2 to form superoxide radical, and thereby enhances oxidative stress (Saito et al. 2011). Thus in chloroplasts, the production of methylglyoxal, an upstream event of ROS production, may be connected via ROS to the formation of RCS.

There are more kinds of carbonyl species that have potential signaling roles in plants (Mueller and Berger 2009, Farmer and Mueller 2013). It appears that each carbonyl species

has a distinct metabolism, i.e. formation and scavenging, and physiological actions. A larger number of experimental facts in broader aspects in plant physiology should be accumulated to build a consistent overview of the signaling action of carbonyls.

We here demonstrate that RCS, downstream products of ROS, can directly activate C1LP and C3LP, and thereby initiate PCD in plant cells, and that they affect the redox homeostasis of cells greatly by consuming GSH. These results provide a specific biochemical explanation for 'plant oxidative injury', the importance of which is widely accepted but the process remains to be clearly described.

3.5 Materials and Methods

3.5.1 Culture of cells

Tobacco BY-2 (*Nicotiana tabacum* L. *cv.* Bright Yellow-2) cell suspension were cultured in Murashige and Skoog medium supplemented with sucrose (30 g l^{-1}), myo-inositol (100 mg l^{-1}), KH_2PO_4 (200 mg l^{-1}), thiamine HCl (0.5 mg l^{-1}) and 2,4-dichlorophenoxyacetic acid (0.2 mg l^{-1}), pH 5.6, with continuous rotation at 120 rpm in darkness at 25°C. The cells were sub-cultured every 7 days; approximately 0.5 mL of cell suspension was transferred to fresh medium (50 ml). Cells in the exponential growth phase, which is established on the fourth day, were used for experiment. Cells were collected by filtration and washed once with distilled water for analyses.

3.5.2 Cell viability assay and protein determination

FDA staining is specific to determine viable cells because only viable cells are able to cleave FDA to form fluorescein and fluoresce with excitation at 485 nm and emission at 515 nm. Dead cells do not fluoresce. Cells were incubated in a solution of FDA (1 μg ml^{-1}) for 5 min and then observed under a fluorescence microscope (Leica AF6000, Wetzlar, Germany) under white and fluorescent light. Protein content was determined with Protein Assay CBB

solution (Nacalai Tesque, Kyoto, Japan) with bovine serum albumin as the standard. Briefly, about 0.4 g cells were harvested and homogenization with extraction buffer (50 mM KH_2PO_4, 1 mM EDTA, 1X Protease Inhibitor Cocktail; pH 7.4). Cell extract centrifuged with 1000 × *g* for 5 min at 4ºC and 0.5 ml supernatant passed through the equilibrated PD MiniTrap G-25 column (GE Healthcare, Tokyo, Japan) to remove small molecules.

3.5.3 Extraction and analysis of glutathione

The glutathione pool was assayed according to de Pinto et al. (1999) with a slight modification. The cells were filtered and washed with distilled water. Chilled with liquid nitrogen, cells (approx. 0.35 g) were ground with a mortar and pestle and two volumes of cold 5% sulphosalicylic acid were added. The homogenate was centrifuged at 20,000 × *g* for 15 min at 4ºC, and the supernatant (cell extract) was collected for analysis. A 0.1 ml aliquot of cell extract was mixed with 0.9 ml of 0.1 M HEPES-KOH, pH 7.4, containing 5 mM EDTA (neutralized cell extract), and divided into two. One fraction was used for determining the total glutathione (GSH + oxidized form (GSSG)) as GSH. The other fraction was for determining GSSG. The concentration of GSH was determined in 1 ml reaction mixture containing 0.1 M HEPES-KOH, pH 7.4, 5 mM EDTA, 10 mM 5,5′-dithiobis-2-nitrobenzoic acid, 0.5 unit glutathione reductase and 0.3 ml of neutralized cell extract. After addition of 0.2 mM NADPH to the reaction mixture the increase rate in A_{412} was recorded for 1 min. A standard curve for GSH in the range of 0-0.1 mM was prepared. For GSSG determination, 20 µl of 2-vinylpyridine was added to the neutralized cell extract and mixed well until emulsion is formed, to mask GSH. After removal of the residual 2-vinylpyridine by centrifugation, GSH concentration was determined as above. The GSH content in the cell was determined as the difference between the amount of total glutathione and that of GSSG.

3.5.4 Extraction and analysis of ascorbate

Asc and DHA were measured according to Kampfenkel et al. (1995) with minor

modifications. Briefly, total ascorbate (Asc + DHA) was determined after reduction of DHA to Asc with DTT, and the concentration of DHA was estimated from the difference between total ascorbate and Asc. Cell extract was prepared in the same way for GSH determination as above. The 1 ml reaction mixture for total ascorbate contained a 0.1 ml aliquot of cell extract, 0.25 ml of 150 mM phosphate, pH 7.4, containing 5 mM EDTA, and 0.05 ml of 10 mM dithiothreitol (DTT). After incubation for 10 min at room temperature, 0.05 ml of 0.5% *N*-ethylmaleimide was added to remove excess DTT. Asc was determined in the same reaction mixture, except that 0.1 ml of H_2O was added rather than DTT and *N*-ethylmaleimide. Color was developed in both reaction mixtures after addition of the following reagents: 0.2 ml of 10% trichloroacetic acid, 0.2 ml of 44% *ortho*-phosphoric acid, 0.2 ml of 4% *α,α*-dipyridyl in 70% ethanol and 0.3% (w/v) $FeCl_3$. After thorough mixing, the mixture was incubated at 40ºC for 40 min and then A_{525} was determined. A standard curve was developed based on Asc in the range of 0-250 μM.

3.5. 5 Determination of C1LP and C3LP activities

Preparation of cell extract and assay of C1LP and C3LP activities was performed as described by Hatsugai et al. (2004). Briefly, 4-d cultured BY-2 cells were harvested, frozen in liquid nitrogen and homogenized with a mortar and pestle in 50 mM sodium acetate, pH 5.5, containing 50 mM NaCl, 1 mM EDTA, 1 mM phenylmethylsulfonyl fluoride and, 0.1 mM E64-d (a thiol protease inhibitor). After centrifugation at 14,000 × *g* for 30 min at 4ºC, the supernatant was collected (cell extract).

C1LP and C3LP activities were measured with synthetic tetrapeptide fluorogenic substrates Ac-YVAD-AMC and Ac-DEVD-AMC (both from Peptide Institute, Osaka, Japan), respectively. Fifty μl of cell extract (or cell-free extract containing 50 μg of protein for Figs. 7 and 8) was mixed with 0.2 ml of reaction mixture containing 20 mM Na-acetate, pH 5.5, 0.1 M DTT, 0.1 mM EDTA and 1 mM phenylmethylsulfonyl fluoride and incubated at 37ºC for 1 h (Hatsugai et al. 2004). Fluorescence of AMC (excitation 380 nm; emission 445 nm) was

determined with a spectrofluorometer (FP-8300, JASCO, Tokyo, Japan). C1LP inhibitor and C3LP inhibitor (Ac-YVAD-CHO and Ac-DEVD-CHO, respectively; Peptide Institute) were added at 0.1 mM to cell extract 1 h before the substrate addition and incubate at 37ºC. Fluorescence intensity difference between the absence and the presence of inhibitor was considered as the activity of the protease. For the detection of *in vitro* activation of C1LP and C3LP, acrolein or H_2O_2 was added to the cell extract and at each time point passed through a PD MiniTrap G-25 column (GE Healthcare, Tokyo, Japan) to remove small molecules. The eluted extracts were added to 0.2 ml reaction mixture as described above. A standard curve was prepared with AMC (Peptide Institute) in the range of 0-200 nM.

3.5.6 ROS detection with H_2DCF-diacetate

BY-2 cells were incubated for 1 h in 0.2 mM acrolein or 0.2 mM acrolein plus 1 mM carnosine, collected by a brief centrifugation and washed with distilled water. They were then incubated with 20 μM H_2DCF-diacetate (Wako Pure Chemical, Osaka, Japan) in PBS at 37°C for 30 min in darkness and washed twice with PBS. The fluorescence was monitored under a fluorescence microscope (Leica LED3000; Leica Microsystems IR GmbH, Wetzlar, Germany) with excitation at 488 nm and emission at 530 nm.

3.5.7 RNA extraction and real time RT-PCR

Total RNA was isolated from the 4-day cultured acrolein treated and untreated BY-2 cells. Cells were harvested and homogenized with a mortar and pestle in liquid nitrogen and RNA was prepared using RNasey Plant Mini Kit (Qiagen, Hilden, Germany). Contaminating genomic DNA was digested with RNase-free DNase (Ambion RNA, Life Technologies, CA, USA). First-strand cDNA was synthesized from 2 μg of total RNA with a ReverTra Ace qPCR kit (Toyobo, Osaka, Japan). Real-time quantitative RT-PCR was carried out using Light Cycler (Roche, Mannheim, Germany) using Thunderbird SYBR qPCR mix (Toyobo, Osaka, Japan). The gene specific-primers and the PCR conditions are listed in Supplemental Table 1. *ACT9* was used to normalize the amount of total transcripts in each sample (Kariya et al. 2013).

3.6 Supplementary data

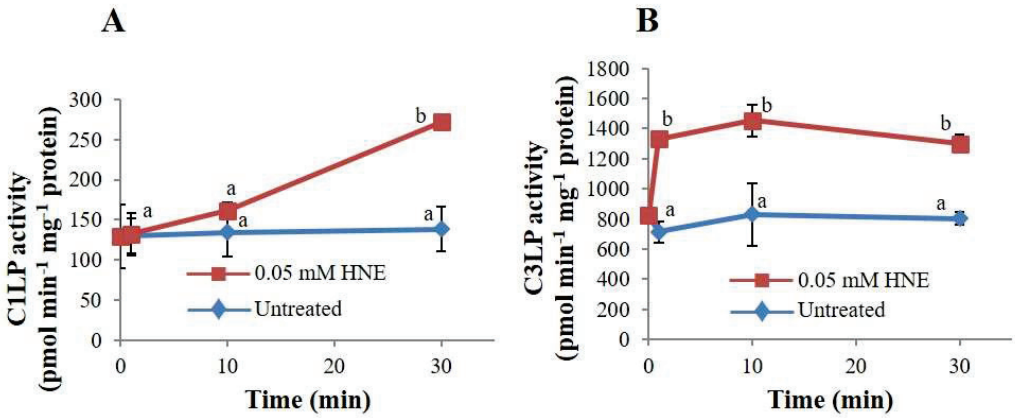

Supplementary Fig. S1 Activation of C1LP and C3LP by HNE in cell-free extract. Total protein was extracted from the 4-day cultured cells. HNE was added and desalting as described in Materials and Methods. Detection of C1LP (A) and C3LP (B) activity after treatment with 0.05 mM HNE. The data are the mean ± SEM. Different letters represent significant different data ($P<0.05$ on Tukey test).

Chapter 4

General discussion

It has been considered that ROS such as superoxide anion radical (O_2^-) and hydrogen peroxide (H_2O_2) acts as central players in the complex signaling network (Mittler *et al.,* 2011) and have been proposed as key inducers of different types of developmental and/or environmental PCD (de Pinto *et al.,* 2012). ROS have generated under oxidative stress drawn full attention for its signaling role in the cell death events of plants. However, the signaling events of ROS are still unclear as to how they transduce signal for the induction of cell death in plants. Plant cellular membranes are abundant sources of lipids, which are direct targets of ROS for oxidation to generate various type of LOOH. A dozens of bioactive carbonyl compounds produced from these LOOH via enzymatic and non-enzymatic ways. Among these carbonyl compounds, the *α,β*-unsaturated carbonyls i.e. RCS, such as acrolein and HNE, have high reactivity and cytotoxicity. Proteins and nucleic acids are sensitive target of carbonyls. They strongly inactivate enzymes in mitochondria and chloroplasts. Therefore, we tested the hypothesis that carbonyls especially RCS induce activation of caspase-like protease starts PCD signals in plants.

We here demonstrated that addition of H_2O_2 to tobacco cells significantly increased several carbonyl compounds such as highly reactive unsaturated carbonyls acrolein and HNE, and the saturated carbonyls *n*-hexenal, *n*-heptanal and propionaldehyde, and (*Z*)-3-hexenal. We found that exogenous application of acrolein, HNE, *n*-hexenal, *n*-heptanal and propionaldehyde that were increased in the H_2O_2 treated tobacco cells efficiently initiated PCD. Interestingly, we observed that saturated carbonyls such as *n*-hexanal and *n*-heptanal also induced cell death but at their higher doses. It demonstrated the potentiality of oxylipin carbonyls to trigger cell death whether it is saturated or unsaturated carbonyls invariably.

The involvement of oxylipin carbonyls in the PCD events also verified in environmental stress responses. For this purpose, H_2O_2 and NaCl-induced cell death was investigated in tobacco cultured cells and in planta. NaCl treatment activates the plasma membrane NADPH

oxidases to facilitate superoxide production, from which H_2O_2 is formed via catalysis with superoxide dismutase. The production of oxylipin carbonyls is closely associated with the presence of ROS. Thus we can expect their involvement in the various physiological processes of plants such as PCD. In the study we used carnosine and hydralazine, having distinct chemistry for scavenging carbonyls, significantly suppressed the increase in oxylipin carbonyls and blocked PCD in BY-2 cells and *A. thaliana* roots. More importantly, the carbonyl scavengers did not affect the levels of ROS and lipid peroxides. In case of genetic study we found that AER-overexpressing tobacco, an Arabidopsis enzyme that detoxify *α,β*-unsaturated carbonyls, suffered less PCD when exposed to H_2O_2 and NaCl. Therefore, the pharmacological and genetic study with the chemical analysis of the involved carbonyls will be a good tool to verify the broader physiological aspects of the carbonyls signal in plant PCD.

Then we investigated the mechanism by which oxylipin carbonyls trigger cell death. We hypothesized that activation of caspase-like protease start cell death signals. Caspase proteases of animals play a central role as PCD regulators to trigger apoptosis in response to various stimuli. The most prevalent executioner caspase in animal cells is caspase-3, which is responsible to switch on cell death (Shi 1999, Kumar 2007). Plants do not have structural homologs of animal caspases, but encode several proteases that share caspase-like activity (Hatsugai et al. 2015, Cai et al. 2014). In plants, C1LP and C3LP activities were identified in many stress and developmental regulated PCD. For example, activation of C1LP was observed in aluminum-induced cell death in tobacco BY-2 cells (Kariya et al. 2013) and C3LP activation was observed in cadmium-induced PCD in *A. thaliana* (Ye et al. 2012). In this study we found that exogenous application of acrolein and HNE activated caspase-like protease and cells went to die. Simultaneously we observed the changes of redox status of the cell after addition of acrolein. We found that activation of caspase-like protease was the earliest events than depletion of glutathione pool and ascorbate contents of the cells. This result suggests that accumulation of oxylipin carbonyls in oxidative stress start PCD by the activation of plant proteases.

Chapter 5

Conclusion

In this study we demonstrated that oxylipin carbonyls, downstream products of ROS, damages cell in oxidative-stressed plants. The involvement of oxylipin carbonyls in the H_2O_2- and NaCl-triggered oxidative signaling was verified by the specific carbonyl scavengers and transgenic tobacco plants that detoxify α,β-unsaturated carbonyls. We aslo examined the mode of cell death that is induced by oxylipin carbonyls, and identified the carbonyl species responsible for the cell death. We found that multiple species of short-chain (C9 or less) oxylipin carbonyls formed in H_2O_2-stimulated cells and they cumulatively contributed to the oxidative signaling, rather than a single very reactive carbonyl such as 4-hydroxy-(*E*)-2-nonenal (HNE). The results demonstrated that the oxylipin carbonyls mediate the oxidative stress-induced PCD in tobacco Bright Yellow-2 (BY-2) cultured cells, and in roots of tobacco and *A. thaliana* plants. We then estimated the relative strengths of distinct carbonyl species to initiate the PCD program. These results demonstrate a critical role of the lipid metabolites in ROS signaling.

Then we investigated the biochemical mechanism by which oxylipin carbonyls trigger cell death. Here we found that RCS can directly activate C1LP and C3LP, and thereby initiate PCD in tobacco BY-2 cells. Acrolein, a member of RCS, rapidly consumes GSH pool and greatly disturbs redox homeostasis of the cells. These results provide a specific biochemical explanation to ‘plant oxidative injury’, of which the importance is widely accepted but the process remains to be clearly described.

References

Aldini G, Carini M, Beretta G, Bradamante S, Facino RM (2002) Carnosine is a quencher of 4-hydroxynonenal: through what mechanism of reaction? Biochem Biophys Res Commun 298: 699–706.

Alméras E, Stolz S, Vollenweider S, Reymond P, Mène-Saffrané L, Farmer EE (2003) Reactive electrophile species activate defense gene expression in *Arabidopsis*. Plant J 34: 205–216.

Apel K, Hirt H (2004) Reactive oxygen species: metabolism, oxidative stress, and signal transduction. Annu Rev Plant Biol 55: 373–399.

Aruoma OI, Laughton MJ, Halliwell B (1989) Carnosine, homocarnosine and anserine: could they act as antioxidants *in vivo*? Biochem J 264: 863–869.

Asada K (2006) Production and scavenging of reactive oxygen species in chloroplasts and their functions. Plant Physiol 141: 391–396.

Asada K (1999) The water-water cycle in chloroplasts: scavenging of active oxygens and dissipation of excess photons. Ann Rev Plant Physiol Plant Mol Biol 50: 601-639.

Bethke PC, Jones RL (2001) Cell death of barley aleurone protoplasts is mediated by reactive oxygen species. Plant J 25: 19–29.

Biswas MS, Mano J (2015) Lipid peroxide-derived short-chain carbonyls mediate hydrogen peroxide-induced and salt-induced programmed cell death in plants. Plant Physiol 168: 885–898.

Burcham PC, Kaminskas LM, Fontaine FR, Petersen DR, Pyke SM (2002) Aldehyde-sequestering drugs: tools for studying protein damage by lipid peroxidation products. Toxicol 181-182: 229–236.

Clarke A, Desikan R, Hurst RD, Hancock JT, and Neill SJ (2000). NO way back: Nitric oxide and programmed cell death in *Arabidopsis thaliana* suspension cultures. Plant J 24: 667–677.

Daiber A, Oelze M, Coldewey M, Kaiser K, Huth C, Schildknecht S, Bachschmid M, Nazirisadeh Y, Ullrich V, Mülsch A, Münzel T, Tsilimingas N (2005) Hydralazine is a powerful inhibitor of peroxynitrite formation as a possible explanation for its beneficial effects on prognosis in patients with congestive heart failure. Biochem Biophys Res Commun 338: 1865–1874.

Dalleau S, Baradat M, Gueraud F, Huc L (2013) Cell death and diseases related to oxidative stress: 4-hydroxynonenal (HNE) in the balance. Cell Death Differ 20:1615–1630.

de Pinto MC, Francis D, De Gara L (1999) The redox state of the ascorbate–dehydroascorbate pair as a specific sensor of cell division in tobacco BY-2 cells. Protoplasma 209: 90–97.

de Pinto MC, Locato V, de Gara L (2012) Redox regulation in plant programmed cell death. Plant Cell Environ 35: 234–244.

del Pozo O, Lam E (1998). Caspases and programmed cell death in the hypersensitive response of plants to pathogens. Curr Biol 8: 1129–1132.

Demidchik V, Cuin TA, Svistunenko D, Smith SJ, Miller AJ, Shabala S, Sokolik A, Yurin V (2010) Arabidopsis root K^+-efflux conductance activated by hydroxyl radicals: single-channel properties, genetic basis and involvement in stress-induced cell death. J Cell Sci 123:1468–1479.

Deng, M., Bian, H., Xie, Y., Kim, Y., Wang, W., Lin, E. et al. (2011) Bcl-2 suppresses hydrogen peroxide-induced programmed cell death via *OsVPE2* and *OsVPE3*, but not via *OsVPE1* and *OsVPE4*, in rice. FEBS J 278: 4797–4810.

Doskočilová A, Kohoutová L, Volc J, Kourová H, Benada O, Chumová J, Plíhal O, Petrovská B, Halada P, Bögre L, Binarová P (2013) *NITRILASE1* regulates the exit from proliferation, genome stability and plant development. New Phytol 198: 685–698.

Esterbauer, H., Zollner, H., Scholz N. (1975) Reaction of glutathione with conjugated carbonyls. *Z.* Naturforsch C 30: 466–473.

Farmer EE, Mueller MJ (2013) ROS-mediated lipid peroxidation and RES-activated signaling.

Annu Rev Plant Biol 64: 429–450.

Fernández MB, Daleo GR, Guevara MG (2012) DEVDase activity is induced in potato leaves during *Phytophthora infestans* infection. Plant Physiol Biochem 61: 197–203.

Foyer CH, Noctor G (2003) Redox sensing and singlling associated with reactive oxygen in chloroplasts, peroxisomes and mitochondria. Physiol Plant 119: 355–364.

Foyer CH, Noctor G (2011) Ascorbate and glutathione: The heart of the redox hub. Plant Physiol 155: 2–18.

Gadjev I, Stone JM, Gechev T (2008) Programmed cell death in plants: new insights into redox regulation and the role of hydrogen peroxide. Intl Rev Cell Mol Biol 270: 87–144.

Gronwald JW, Plaisance KL (1998) Isolation and characterization of glutathione S-transferase isozymes from sorghum. Plant Physiol 117: 877–892.

Grosch W (1987) Reactions of hydroperoxides — products of low molecular weight, in: H.W.-S. Chan (Ed.), Autoxidation of Unsaturated Lipids, Academic Press, London. pp. 95–139.

Halliwell B, Gutteridge JMC (2007) Free Radicals in Biology and Medicine, Fourth edition, Oxford University Press, Oxford.

Han JJ, Lin W, Oda Y, Cui KM, Fukuda H (2012) The proteasome is responsible for caspase-3-like activity during xylem development. Plant J 72: 129–141.

Hatsugai N, Kuroyanagi M, Yamada K, Meshi T, Tsuda S, Kondo M, Nishimura M, Hara-Nishimura I (2004) A plant vacuolar protease, VPE, mediates virus-induced hypersensitive cell death. Science 305: 855–858.

Hatsugai N, Iwasaki S, Tamura K, Kondo M, Fuji K, Ogasawara K, Nishimura M, Hara-Nishimura I (2009) A novel membrane fusion-mediated plant immunity against bacterial pathogens. Genes Dev 23: 2496–2506.

Hatsugai N, Yamada K, Goto-Yamada S, Hara-Nishimura I (2015) Vacuolar processing enzyme in plant programmed cell death. Front Plant Sci 6: 234.

He X, Kermode AR (2003) Programmed cell death of the megagametophyte during post-germinative growth of white spruce (*Picea glauca*) seeds is regulated by reactive oxygen species and the ubiquitin-mediated proteolytic system. Plant Cell Physiol 51: 1707–1720.

Hideg É, Nagy T, Oberschall A, Dudits D, Vass I (2003) Detoxification function of aldose/aldehyde redutase during drought and ultraviolet-B (280-320 nm) stresses. Plant Cell. Environ 26: 513–522.

Higdon A, Diers AR, Oh JY, Landar A, Darley-Usmar VM (2012) Cell signalling by reactive lipid species: new concepts and molecular mechanisms. Biochem J 442: 453–464.

Hogg BV, Kacprzyk J, Molony EM, O'Reilly C, Gallagher TF, Gallois P, McCabe PF (2011) An *in vivo* root hair assay for rates of apoptotic-like programmed cell death in plants. Plant Methods 7: 45.

Houot V, Etienne P, Petitot AS, Barbier S, Blein JP, Suty L (2001) Hydrogen peroxide induces programmed cell death features in cultured tobacco BY-2 cells, in a dose-dependent manner. J Exp Bot 52: 1721–1730.

Islam MM, Ye W, Matsushima D, Khokon MA, Munemasa S, Nakamura Y, Murata Y (2015) Inhibition by acrolein of light-induced stomatal opening through inhibition of inward-rectifying potassium channels in *Arabidopsis thaliana*. Biosci Biotechnol Biochem 79: 59–62.

Kai H, Hirashima K, Matsuda O, Ikegami H, Winkelmann T, Nakahara T, Iba K (2012) Thermotolerant cyclamen with reduced acrolein and methyl vinyl ketone. J Exp Bot 63:4143-4150.

Kampfenkel K, Montagu MV, Inzé D (1995) Extraction and determination of ascorbate and dehydroascorbate from plant tissue. Anal Biochem 225: 165–167

Kariya K, Demiral T, Sasaki T, Tsuchiya Y, Turkan I, Sano T, Hasezawa S, Yamamoto Y (2013) A novel mechanism of aluminium-induced cell death involving vacuolar

processing enzyme and vacuolar collapse in tobacco cell line BY-2. J Inorg Biochem 128: 196–201.

Khorobrykh SA, Khorobrykh AA, Yanykin DV, Ivanov BN, Klimov VV, Mano J (2011) Photoproduction of catalase-insensitive peroxides on the donor side of manganese-depleted photosystem II: evidence with a specific fluorescent probe. Biochem 50: 10658–10665.

Kirch HH, Nair A, Bartels D (2001) Nobel ABA- and dehydration-inducible aldehyde dehydrogenase genes isolated from the resurrection plant *Craterostigma plantagineum* and *Arabidopsis thaliana*. Plant J 28: 555–567.

Kotchoni SO, Kuhns C, Ditzer A, Kirch H-H, Bartels D (2006) Overexpression of different aldehyde dehydrogenase genes in *Arabidopsis thaliana* confers tolerance to abiotic stress and protects plants against lipid peroxidation and oxidative stress. Plant Cell Environ 29: 1033–1048.

Kruman I, Bruce-Keller AJ, Bredesen D, Waeng G, Mattson MP (1997) Evidence that 4-hydroxynonenal mediates oxidative stress-induced neuronal apoptosis. J Neurosci 17: 5089–5100.

Kuriyama H, Fukuda H (2002) Developmental programmed cell death in plants. Curr Opin Plant Biol 5: 568–573.

Levine A, Tenhaken R, Dixon R, Lamb CJ (1994) H_2O_2 from the oxidative burst orchestrates the plant hypersensitive disease resistance response. Cell 79: 583–593.

Liu-Snyder P, Borgens RB, Shi R (2006) Hydralazine rescues PC12 cells from acrolein-mediated death. J Neurosci Res 84: 219–227.

Locato V, Gadaleta C, De Gara L, de Pinto MC (2008) Production of reactive species and modulation of antioxidant network in response to heat shock: a critical balance for cell fate. Plant Cell Environ 31: 1606–1619.

Lombardi L, Ceccarelli N, Picciarelli P, Sorce C, Lorenzi R (2010) Nitric oxide and hydrogen

peroxide involvement during programmed cell death of Sechium edule nucellus. Physiol Plant 140: 89–102.

Maeda H (2008) Which are you watching, an individual reactive oxygen species or total oxidative stress? Ann N Y Acad Sci 1130:149–56.

Mano J (2002) Early events in environmental stresses in plants — Induction mechanisms of oxidative stress. In D. Inzé and M. Van Montagu, eds., Oxidative Stress in Plants, pp. 217-245, Taylor & Francis Group, London.

Mano J, Belles-Boix E, Babiychuk E, Inzé D, Torii Y, Hiraoka H, Takimoto K, Slooten L, Asada K, Kushnir S (2005) Protection against photooxidative injury of tobacco leaves by 2-alkenal reductase. Detoxication of lipid peroxide-derived reactive carbonyls. Plant Physiol 139: 1773–1783.

Mano J, Miyatake F, Hiraoka E, Tamoi M (2009) Evaluation of the toxicity of stress related aldehydes to photosynthesis in chloroplasts. Planta 230: 639–648.

Mano J, Tokushige K, Mizoguchi H, Fujii H, Khorobrykh S (2010) Accumulation of lipid peroxide-derived, toxic α,β-unsaturated aldehyde (*E*)-2-pentenal, acrolein and (*E*)-2-hexenal in leaves under photoinhibitory illumination. Plant Biotechnol 27: 193–197.

Mano J (2012) Reactive carbonyl species: Their production from lipid peroxides, action in environmental stress, and the detoxification mechanism. Plant Physiol Biochem 59: 90–97.

Mano J, Khorobrykh S, Matsui K, Iijima Y, Sakurai N, Suzuki H, Shibata D (2014a) Acrolein is formed from trienoic fatty acids in chloroplasts: A targeted metabolomics approach. Plant Biotechnol 31: 535-543.

Mano J, Nagata M, Okamura S, Shiraya T, Mitsui T (2014b) Identification of oxidatively modified proteins in salt-stressed Arabidopsis: a carbonyl-targeted proteomics approach. Plant Cell Physiol 55: 1233–1244.

Mano J, Torii Y, Hayashi S, Takimoto K, Matsui K, Nakamura K, Inzé D, Babiychuk E,

Kushnir S, Asada K (2002) The NADPH:quinone oxidoreductase P1-ζ-crystallin in Arabidopsis catalyzes the *α,β*-hydrogenation of 2-alkenals: detoxification of the lipid peroxide-derived reactive aldehydes. Plant Cell Physiol 23: 1445–1455.

Matsui K, Sugimoto K, Kakumyan P, Khorobrykh SA, Mano J (2009) Volatile oxylipins and related compounds formed under stress in plants. In D. Armstrong, ed., Methods in Molecular Biology, 'Lipidomics' 580: 17–28.

Matsui K, Sugimoto K, Mano J, Ozawa R, Takabayashi J (2012) Differential metabolism of green leaf volatiles in injured and intact parts of a wounded leaf meet distinct ecophysiological requirements. PLoS One 7: e36433.

Mène-Saffrané L, Davoine C, Stolz S, Majcherczyk P, Farmer EE (2007) Genetic removal of tri-unsaturated fatty acids suppresses developmental and molecular phenotypes of an Arabidopsis tocopherol-deficient mutant. J Biol Chem 282: 35749–35756.

Miller G, Suzuki N, Ciftci-Yilmaz S, Mittler, R (2010) Reactive oxygen species homeostasis and signalling during drought and salinity stresses. Plant Cell Environ 33: 453–467.

Mittler R, Vanderauwera S, Suzuki N, Miller G, Tognetti VB, Vandepoele K, Gollery M, Shulaev V, Breusegem FV (2011) ROS signaling: the new wave? Trends Plant Sci 16: 300–309.

Møller IM, Sweetlove LJ (2010) ROS signalling—specificity is required. Trends Plant Sci 15: 370–374.

Monetti E, Kadono T, Tran D, Azzarello E, Arbelet-Bonnin D, Biligui B, Briand J, Kawano T, Mancuso S, Bouteau F (2014) Deciphering early events involved in hyperosmotic stress-induced programmed cell death in tobacco BY-2 cells. J Exp Bot 65: 1361–1375.

Montillet J-L, Cacas J-L, Cariner L, Montané M-H, Douki T, Beseoule J-J, Plokowska-Kowalczyk L, Maciejewska U, Agnael J-P, Vial A, Trantaphylidès C (2004) The upstream oxylipin profile of *Arabidopsis thaliana*: a tool to scan for oxidative stresses. Plant J 40: 439-451.

Mueller MJ, Berger S (2009) Reactive electrophile oxylipins: Pattern recognition and signaling. Phytochemistry 70: 1511–1521.

Nagata T, Sakamoto K, Shimizu T (2004) Tobacco BY-2 cells: the present and beyond. In Vitro Cell Dev Biol-Plant 40: 163–166.

Nakagami H, Soukupova H, Schikora A, Zarsky V, Hirt H (2006) A mitogen-activated protein kinase kinase kinase mediates reactive oxygen species homeostasis in Arabidopsis. J Biol Chem 281:38697–38704.

Nguyen GN, Hailstones DL, Wilkes M, Sutton BG (2009) Drought-induced oxidative conditions in rice anthers leading to a programmed cell death and pollen abortion. J Agr Crop Sci 195: 157–164.

Oberschall A, Deák M, Török K, Sass L, Vass I, Kocács I, Fehér A, Dudits D, Horváth GV (2000) A novel aldose/aldehyde reductase protects transgenic plants against lipid peroxidation under chemical and drought stress. Plant J 24: 437–446.

Park SW, Li W, Viehhauser A, He B, Kim S, Nilsson AK, Andersson MX, Kittle JD, Ambavaram MM, Luan S, Esker AR, Tholl D, Cimini D, Ellerström M, Coaker G, Mitchell TK, Pereira A, Dietz KJ, Lawrence CB (2013) Cyclophilin 20-3 relays a 12-oxo-phytodienoic acid signal during stress responsive regulation of cellular redox homeostasis. Proc Natl Acad Sci 110: 9559–9564.

Pei ZM, Murata Y, Benning G, Thomine S, Klüsener B, Allen GJ, Grill E, Schroeder, JI (2000) Calcium channels activated by hydrogen peroxide mediate abscisic acid signalling in guard cells. *Nature* 406:731–734.

Pennell RI, Lamb C (1997) Programmed cell death in plants. Plant Cell 9: 1157–1168.

Petrov V, Hille J, Mueller-Roeber B, Gechev TS (2015) ROS-mediated abiotic stress-induced programmed cell death in plants. Front Plant Sci 6: 69.

Petrov V, Hille J, Mueller-Roeber B, Gechev TS (2015) ROS-mediated abiotic stress-induced programmed cell death in plants. Front Plant Sci 6: 69.

Reape TJ, McCabe PF (2008) Apoptotic-like programmed cell death in plants. New Phytol 180: 13–26.

Rodríguez-Serrano M, Bárány I, Prem D, Coronado M, Risueño MC, Testillano PS (2011) NO, ROS, and cell death associated with caspase-like activity increase in stress-induced microspore embryogenesis of barley. J Exp Bot 63: 2007–2024.

Saito R, Yamamoto H, Makino A, Sugimoto T, Miyake C (2011) Methylglyoxal functions as hill oxidant and stimulates the photoreduction of O_2 at photosystem I: a symptom of plant diabetes. Plant Cell Environ 34: 1454–1464.

Shi Y (2002) Mechanisms of caspase activation and inhibition during apoptosis. Mol Cell 9: 459–470.

Shi Y (2004) Caspase activation: Revisiting the induced proximity model. Cell 117: 855–858.

Shin JH, Kim SR, An G (2009) Rice Aldehyde Dehydrogenase7 is needed for seed maturation and viability. Plant Physiol 149: 905–915.

Soh N, Ariyoshi T, Fukaminato T, Nakajima H, Nakano K, Imato T (2007) Swallow-tailed perylene derivative: A new tool for fluorescent imaging of lipid hydroperoxides. Org Biomol Chem 5: 3762−3768.

Sun J, Okumura H, Yearsley M, Frankel W, Fong LY, Druck T, Huebner K (2009) Nit1 and Fhit tumor suppressor activities are additive. J Cell Biochem 107: 1097−1106.

Sunker R, Bartels D, Kirch H-H (2003) Overexpression of a stress-inducible aldehydes dehydrogenase gene from Arabidopsis thaliana in transgenic plants improves stress tolerance. Plant J 35: 452−464.

Suzuki N, Rivero RM, Shulaev V, Blumwald E, Mittler R (2014) Abiotic and biotic stress combinations. New Phytol 203: 32–43.

Takagi D, Inoue H, Odawara M, Shimakawa G, Miyake C (2014) The Calvin cycle inevitably produces sugar-derived reactive carbonyl methylglyoxal during photosynthesis: a potential cause of plant diabetes. Plant Cell Physiol 55: 333–340.

Tang W, Sun J, Liu J, Liu F, Yan J, Gou X, Lu B-R, Liu Y (2014) RNAi-directed downregulation of *betaine aldehyde dehydrogenase 1* (*OsBADH1*) results in decreased stress tolerance and increased oxidative stress markers without affecting glycine betaine biosynthesis in rice (*Oryza sativa*). Plant Mol Biol 86: 443–454.

Taylor NL, Day DA, Millar AH (2002) Environmental stress causes oxidative damage to plant mitochondria leading to inhibition of glycine decarboxylase. J Biol Chem 277: 42662–42668.

Torres MA, Jones JD, Dangl JL (2005) Pathogen-induced, NADPH oxidase-derived reactive oxygen intermediates suppress spread of cell death in *Arabidopsis thaliana*. Nat Genet 37: 1130–1134.

Torres MA, Dangl JL (2005) Functions of the respiratory burst oxidase in biotic interactions, abiotic stress and development. Curr Opin Plant Biol 8: 397–403.

Tsukagoshi H, Busch W, Benfey PN (2010) Transcriptional regulation of ROS controls transition from proliferation to differentiation in the root. Cell 143: 606–616.

Vacca RA, Valenti D, Bobba A, de Pinto MC, Merafina RS, De Gara L, Passarella S, Marra E (2007) Proteasome function is required for activation of programmed cell death in heat shocked tobacco Bright-Yellow 2 cells. FEBS Letters 581: 917–922.

Van Breusegem F, Dat JF (2006) Reactive oxygen species in plant cell death. Plant Physiol 141: 384–90.

Winger AM, Taylor NL, Heazlewood JL, Day DA, Millar AH (2007) The cytotoxic lipid peroxidation product 4-hydroxy-2-nonenal covalently modifies a selective range of proteins linked to respiratory function in plant mitochondria. J Biol Chem 282: 37436–37447.

Xu FJ, Jin CW, Liu WJ, Zhang YS, Lin XY (2011) Pretreatment with H_2O_2 alleviates aluminum-induced oxidative stress in wheat seedlings. J Integr Plant Biol 53:44–53.

Yamauchi Y, Hasegawa A, Mizutani M, Sugimoto Y (2012) Chloroplastic NADPH dependent

alkenal/one oxidoreductase contributes to the detoxification of reactive carbonyls produced under oxidative stress. FEBS Letters 586: 1208–1213.

Yamauchi Y, Kunishima M, Mizutani M, Sugimoto Y (2015) Reactive short-chain leaf volatiles act as powerful inducers of abiotic stress-related gene expression. Sci Rep 5: 8030.

Ye Y, Li Z, Xing D (2013) Nitric oxide promotes MPK6-mediated caspase-3-like activation in cadmium-induced Arabidopsis thaliana programmed cell death. Plant Cell Environ 36: 1–15.

Yin L, Mano J, Wang S, Tsuji W, Tanaka K (2010) The involvement of lipid peroxide-derived aldehydes in aluminum toxicity of tobacco roots. Plant Physiol 152: 1406–1417.

Yoda H, Yamaguchi Y, Sano H (2003) Induction of hypersensitive cell death by hydrogen peroxide produced through polyamine degradation in tobacco plants. Plant Physiol 132: 1973–1981.

Zapata JM, Guéra A, Esteban-Carrasco A, Martín M, Sabater B (2005) Chloroplasts regulate leaf senescence: delayed senescence in transgenic ndhF-defective tobacco. Cell Death Differ 12: 1277–1284.

Acknowledgements

First of all, I would like to thank my supervisor Prof. Dr. Jun'ichi Mano for giving me the opportunity to work on the exciting project of oxylipin carbonyls signals in the plant physiological process. Furthermore, I appreciate that he always had a sympathetic mind for any scientific problem. Moreover, I am grateful for his valuable advice, thoughtful comments and scientific support in any way.

I am grateful to Prof. Dr. Kenji Matsui for his help and discussion throughout whole PhD research. In particular, I would like to thank him for his critical discussion in the progress seminar. As well as many thanks to the whole laboratory members of Prof. Matsui which made the environment a lot more comfortable with their cheerfulness. A special thank I would like to offer Prof. Atsushi Sakamoto, Hiroshima University for providing me the research material tobacco BY-2 cells.

Many thanks to my old and new colleagues Nagata, Okamura, Hirota, Ishibashi, Yamamoto, Iwanaga, Tokunaga, Sakai, Shibutani, Hashimoto, Tasaki who made the lab atmosphere so friendly and familiar. Especially I would like to thank Ito of my old lab member and Kida Miuzu for their support with any kind of private and business issues.

I am indebted to the Japan Ministry of Education, Culture, Sports, Science and Technology (Monbukagakusho) for providing financial support for my study. Without this support, I would not have been able to accomplish this work. Kaze-no-kai, a local organization of Yamaguchi also made my life enjoyable, many thanks to them.

Above all I would like to thank my parents and parents-in-law for their never ending support during my PhD years. I also received a lot of inspiration from my elder brother Azad Rahman for timely accomplishment of my course. My sister-in-law Taposi also supported me to raise my child. Finally, but most important I would like to say thanks to my wife Atika Zinia who always supported me in my aim of being a PhD as well as many thanks to my only son Zayed who struggle a lot at his very early age.

Md. Sanaullah Biswas
September 2016

和文要旨

活性酸素（ROS）によって引き起こされるプログラム細胞死（PCD）は，植物の生物的ストレスや環境ストレスに対する応答のなかでも典型的なものである。過酸化脂質分解産物であり有毒なカルボニル化合物（オキシリピンカルボニル）はROSの下流の代謝産物であり，植物のストレス傷害の原因物質であることが最近明らかになってきた。本研究ではまずオキシリピンカルボニルが酸化シグナルとして植物のPCDを引き起こす可能性を検証した。タバコBright Yellow-2（BY-2）培養細胞にH_2O_2を与えると，4-ヒドロキシノネナールやアクロレインといった短鎖オキシリピンカルボニルの含量が増大した。このときDNA断片化，TUNEL陽性細胞核の増大および細胞質収縮観察を基にPCDが進行することを明らかにした。タバコおよびシロイヌナズナの根にH_2O_2またはNaClを与えた実験で，植物体でもオキシリピンカルボニルがPCDを引き起こすことを明らかにした。H_2O_2により生じる BY-2細胞のPCDは，カルボニル化合物消去剤であるカルノシンやヒドララジンにより抑制された。これらの消去剤はH_2O_2による細胞内でのROS増大や過酸化脂質増大を抑制しなかった。またNaClにより誘導される根表皮のPCDは，α,β-不飽和カルボニル種を特異的に消去するシロイヌナズナ酵素 2-alkenal reductaseの過剰発現により抑制された。この過剰発現株でのROS増大は野生株と同程度であった。これらの結果から，ROSの下流で生成したオキシリピンカルボニルがPCDを開始させるシグナルとして作用することが示された。

PCD開始時のオキシリピンカルボニルの作用を解明するため，代表的なカルボニル化合物としてアクロレインを用い，BY-2細胞にPCDを引き起こす致死濃度（0.2 mM）または引き起こさない亜致死濃度（0.1 mM）のアクロレイン与え，生化学変化の差を解析した。PCDに関与するカスパーゼ3様プロテアーゼ（C3LP）は，致死濃度アクロレインでは急速に活性化されたが，亜致死濃度では最大値の半分までしか活性化されなかった。致死濃度ではアスコルビン酸含量が有意に低下したが，これはC3LP活性化より遅い現象であった。細胞内のグルタチオン含量はアクロレイン添加により急速に減少したが，亜致死濃度，致死濃度での違いはなく，PCDの開始に直接関係はないことが分かった。BY-2細胞の抽出液にアクロレインまたはHNEを加えるとC3LP活性が急速に増大したが，H_2O_2はC3LPを活性化しなかった。すなわち，H_2O_2投与により細胞内のC3LP活性が増大したのは，H_2O_2の直接作用ではなく，下流で作られたアクロレインなどのオキシリピンカルボニルの作用によることが示された。以上の結果から，植物において酸化シグナルの伝達には脂質酸化代謝物が重要な役割を果たしていることを立証した。

List of publication

1. Title : **Lipid peroxide-derived short-chain carbonyls mediate H_2O_2-induced and NaCl-induced programmed cell death in plants**

   Authors : Md. Sanaullah Biswas and Jun'ichi Mano

   Journal : Plant Physiology

   Date : July 2015

   This paper covers Chapter 2 of this thesis

2. Title : **Reactive carbonyl species activate caspase-3-like protease to initiate programmed cell death in plants**

   Authors : Md. Sanaullah Biswas and Jun'ichi Mano

   Journal : Plant and Cell Physiology

   Date : April 2016

   This paper covers Chapter 3 of this thesis